Neuroscience 250 (2013) 755–772

VOLTAGE-GATED Ca^{2+} INFLUX AND MITOCHONDRIAL Ca^{2+} INITIATE SECRETION FROM *APLYSIA* NEUROENDOCRINE CELLS

C. M. HICKEY, C. J. GROTEN, L. SHAM, C. J. CARTER AND N. S. MAGOSKI *

Department of Biomedical and Molecular Sciences, Queen's University, Kingston, ON K7L 3N6, Canada

Abstract—Neuroendocrine secretion often requires prolonged voltage-gated Ca^{2+} entry; however, the ability of Ca^{2+} from intracellular stores, such as endoplasmic reticulum or mitochondria, to elicit secretion is less clear. We examined this using the bag cell neurons, which trigger ovulation in *Aplysia* by releasing egg-laying hormone (ELH) peptide. Secretion from cultured bag cell neurons was observed as an increase in plasma membrane capacitance following Ca^{2+} influx evoked by a 5-Hz, 1-min train of depolarizing steps under voltage-clamp. The response was similar for step durations of $\geqslant$50 ms, but fell off sharply with shorter stimuli. The capacitance change was attenuated by replacing external Ca^{2+} with Ba^{2+}, blocking Ca^{2+} channels, buffering intracellular Ca^{2+} with EGTA, disrupting synaptic protein recycling, or genetic knock-down of ELH. Regarding intracellular stores, liberating mitochondrial Ca^{2+} with the protonophore, carbonyl cyanide-*p*-trifluoromethoxyphenylhydrazone (FCCP), brought about an EGTA-sensitive elevation of capacitance. Conversely, no change was observed to Ca^{2+} released from the endoplasmic reticulum or acidic stores. Prior exposure to FCCP lessened the train-induced capacitance increase, suggesting overlap in the pool of releasable vesicles. Employing GTP-γ-S to interfere with endocytosis delayed recovery (presumed membrane retrieval) of the capacitance change following FCCP, but not the train. Finally, secretion was correlated with reproductive behavior, in that neurons isolated from animals engaged in egg-laying presented a greater train-induced capacitance elevation vs quiescent animals. The bag cell neuron capacitance increase is consistent with peptide secretion requiring high Ca^{2+}, either from influx or stores, and may reflect the all-or-none nature of reproduction.

Key words: capacitance, calcium channel, FCCP, CPA, bag cell neurons, peptide release.

INTRODUCTION

Like classical neurotransmission, peptide and neuroendocrine secretion depends on Ca^{2+} influx (Neher, 1998). There is often a delay between voltage-gated Ca^{2+} entry and peptide release, suggesting a Ca^{2+} threshold for secretion (Thomas et al., 1993; Hsu and Jackson, 1996; Branchaw et al., 1998; Sedej et al., 2004). Prolonged periods of action potentials or membrane depolarization are typically more effective than short stimuli at triggering neuropeptide secretion, presumably because this elevates Ca^{2+} over the threshold (Dreifuss et al., 1971; Bicknell and Leng, 1981; Hartzell, 1981; Gainer et al., 1986; Lim et al., 1990; Soldo et al., 2004). In addition, Ca^{2+} from stores can bring intracellular Ca^{2+} closer to the threshold and directly or indirectly influence peptide release (Ammälä et al., 1993; Tse et al., 1997; Shakiryanova et al., 2007; Gilbert et al., 2008). Overall, a threshold may limit hormonally-induced behaviors, particularly high-priority fixed-action patterns that proceed to completion once initiated (Kupfermann and Weiss, 1978).

The bag cell neurons of the marine mollusk, *Aplysia californica*, are neuroendocrine cells that control reproduction through a long-term change in excitability known as the afterdischarge (Kupfermann, 1967; Conn and Kaczmarek, 1989). This burst results from cholinergic and peptidergic inputs, and consists of a fast phase (5-Hz firing for approximately 1 min) and a slow phase (1-Hz firing sustained over 30 min) (Kaczmarek et al., 1982; Brown et al., 1989; White and Magoski, 2012). Intracellular Ca^{2+} rises sharply during the fast phase (Fisher et al., 1994; Michel and Wayne, 2002). *In vivo*, this leads to the neurohaemal release of several peptides, including egg-laying hormone (ELH), which act on central and peripheral targets to evoke egg-laying behavior (Dudek and Tobe, 1978; Chiu et al., 1979; Stuart et al., 1980). Biochemical techniques have revealed Ca^{2+}-dependent peptide secretion from bag

*Corresponding author. Address: Department of Biomedical and Molecular Sciences, Queen's University, 4th Floor, Botterell Hall, 18 Stuart Street, Kingston, ON K7L 3N6, Canada. Tel: +1-613-533-2700; fax: +1-613-533-6880.
E-mail address: magoski@queensu.ca (N. S. Magoski).

Abbreviations: ATP, adenosine triphosphate; Ba^{2+}-Cs^{+}-TEA ASW, Ba^{2+}, Cs^{+} tetraethylammonium artificial sea water; Baf, bafilomycin A; Ca^{2+}-Cs^{+}-TEA ASW, Ca^{2+}, Cs^{+} tetraethylammonium artificial sea water; cfASW, Ca^{2+}-free artificial salt water; C_m, membrane capacitance; Cntl, control; CPA, cyclopiazonic acid; DMSO, dimethyl sulfoxide; dsRNA, double-stranded ribonucleic acid; EGTA, ethyleneglycol bis (aminoethylether) tetraacetic acid; ELH, egg-laying hormone; EtOH, ethanol; FCCP, carbonyl cyanide-*p*-trifluoromethoxyphenyl-hydrazone; GTP, guanosine triphosphate; GTP-γ-S, guanosine-5′-[γ-thio]triphosphate; HEPES, *N*-2-hydroxyethlpiperazine-N′-2-ethanesulphonic acid; I_b, baseline current; IgG, immunogammaglobulin; I_{ss}, steady-state current; MEM, minimum essential medium; nASW, normal artificial salt water; NEM, N-ethylmaleimide; PBS, phosphate-buffered saline; Q_{cf}, correction factor charge; Q_t, total charge; Q_{tc}, charge during transient current; R_a, access resistance; R_m, membrane resistance; SEM, standard error of the mean; tcASW, tissue culture artificial salt water; TEA, tetraethylammonium; TFA, trifluoroacetic acid; TRIS, 2-amino-2-hydroxymethyl-propane-1,3-diol; ΔI, current change to a voltage step; ΔV, step voltage; τ, membrane time constant.

0306-4522/13 $36.00
http://dx.doi.org/10.1016/j.neuroscience.2013.07.023

cell neurons in the intact nervous system following an afterdischarge or high extracellular K^+-mediated depolarization (Arch, 1972; Loechner et al., 1990, 1992; Michel and Wayne, 2002; Hatcher and Sweedler, 2008). The peptides expressed by bag cell neurons are also preserved *in vitro* (Chiu and Stumwasser, 1981), and mass spectrometry has shown ELH release from cultured bag cell neurons subsequent to action potential firing (Hatcher et al., 2005; Jo et al., 2007).

The afterdischarge, neuropeptide secretion, and egg-laying behavior are effectively all-or-none events (Kupfermann, 1967; Ferguson et al., 1989). Yet the relationship between afterdischarge duration and the volume of eggs deposited is less than linear, i.e., even bursts that are shorter than 30 min result in eggs (Dudek et al., 1979). This likely involves the release of Ca^{2+} from intracellular stores promoting ELH secretion subsequent to the afterdischarge (Michel and Wayne, 2002). These circumstances, in combination with the fact that most work on secretion has used the intact cluster, have made it difficult to resolve what duration or pattern of activity is sufficient to cause secretion. Thus, the aim of the present study was to use voltage-clamp and capacitance tracking to characterize how Ca^{2+} entry or release elicits secretion in real time from individual cultured bag cell neurons. Our findings show that only prominent Ca^{2+} elevation, either due to voltage-gated influx or liberation from the mitochondria, initiates secretion. Such conditions fit with a behavior that is fundamental to survival, and may reflect a general principal for the neuroendocrine control of high-threshold actions.

EXPERIMENTAL PROCEDURES

Animals and cell culture

Primary cultures of isolated bag cell neurons were obtained from adult 150–500 g *A. californica* (a hermaphrodite) purchased from Marinus (Long Beach, CA, USA) or Santa Barbara Marine Biologicals (Santa Barbara, CA, USA) and housed in an approximate 300-l aquarium containing continuously circulating, aerated artificial seawater (Instant Ocean; Aquarium Systems; Mentor, OH, USA) at 14–16 °C on 12/12-h light/dark cycle and fed Romaine lettuce 5×/week. All experiments were approved by the Queen's University Animal Care Committee (Protocol No. 100323-Magoski-2012). Following anesthesia by injection of isotonic $MgCl_2$ (around 50% of body weight), the abdominal ganglion was removed and treated for 18 h with neutral protease (13.33 mg/ml; 165859; Roche Diagnostics, Indianapolis, IN, USA) dissolved in tissue culture artificial seawater (tcASW; containing in mM: 460 NaCl, 10.4 KCl, 11 $CaCl_2$, 55 $MgCl_2$, 10 4-(2-hydroxyethyl)-1-piperazineethanesulfonic acid (HEPES), glucose (1 mg/ml), penicillin (100 U/ml), and streptomycin (0.1 mg/ml), pH 7.8 with NaOH). The ganglion was then transferred to fresh tcASW and the two-bag cell neuron clusters dissected from their surrounding connective tissue. Using a fire-polished Pasteur pipette and gentle trituration, neurons were dispersed in simple culture medium (as per tcASW plus minimum essential medium (MEM) vitamins (0.5×; 11120052; Gibco/Invitrogen; Grand Island, NY, USA), MEM non-essential amino acids (0.2×; 11400050; Gibco/Invitrogen), and MEM essential amino acids without L-glutamine (0.2×; 1130051; Gibco/Invitrogen) onto 35 × 10 mm polystyrene tissue culture dishes (430165; Corning, Corning, NY, USA or 353001; Ulti-Dent Scientific, St.-Laurent, QC, Canada) and maintained for 1–3 d in a 14 °C incubator. Experiments were carried out at 22 °C. Salts were from Fisher Scientific (Ottawa, ON, Canada), ICN (Irvine, CA, USA), or Sigma–Aldrich (St. Louis, MO, USA).

Whole-cell voltage-clamp recording

Voltage-clamp recordings were made using an EPC-8 amplifier (HEKA Electronics; Mahone Bay, NS, Canada) and the tight-seal, whole-cell method. Microelectrodes were pulled from 1.5 mm external diameter/1.12 internal diameter, borosilicate glass capillaries (TW150F-4; World Precision Instruments, Sarasota, FL, USA) and had a resistance of 1–3 MΩ when filled with various intracellular salines (see below). Pipette junction potentials were nulled immediately before seal formation, while pipette capacitive currents were canceled immediately after break through. To facilitate membrane capacitance tracking (see below), series resistance and whole-cell capacitance were usually not compensated. However, Ca^{2+} currents were occasionally measured separate from capacitance, and in those cases the series resistance (2–5 MΩ) was compensated to 70–80% and monitored throughout the experiment, while the neuronal capacitance was canceled by the whole-cell capacitance compensation. Current was filtered at 1 kHz by the EPC-8 built-in Bessel filter and sampled at 2 kHz using an IBM-compatible personal computer, a Digidata 1300 analog-to-digital converter (Axon Instruments/Molecular Devices; Sunnyvale, CA, USA) and the Clampex acquisition program of pCLAMP 8.1 (Axon Instruments). Clampex was also used to set the holding and command potentials.

In most cases, neurons were held at −80 mV and stimulated with a 5-Hz, 1-min train of square voltage pulses to 0 mV to produce Ca^{2+} influx and secretion (see Results for details). Subtraction of leak from the train-induced Ca^{2+} currents was achieved by subsequently blocking Ca^{2+} channels with 10 mM Ni^{2+}, delivering the train a second time, then subtracting the current in Ni^{2+} from the control current (as per Hung and Magoski, 2007; Tam et al., 2009). In some experiments, neurons were held at −60 mV and Ca^{2+} currents evoked with 200-ms square pulses from −60 mV to +40 mV in 10-mV increments. Leak subtraction from these currents was performed on-line using a *P*/4 protocol from −60 mV with subpulses of opposite polarity and one-fourth the magnitude, an inter-subpulse interval of 500 ms, and 100 ms before actual test pulses.

Most recordings were performed in Ca^{2+}-Cs^{+}-TEA ASW, where NaCl and KCl were replaced by TEA-Cl and CsCl, respectively (composition in mM: 460 TEA-Cl, 10.4 CsCl, 55 $MgCl_2$, 11 $CaCl_2$, 15 HEPES, pH 7.8 with CsOH). This was paired with a Cs^{+}-aspartate-based intracellular saline (composition in mM: 70 CsCl, 10 HEPES, 11 glucose, 10 glutathione, 5 ethyleneglycol bis(aminoethylether) tetraacetic acid (EGTA), 500 aspartic acid, 5 ATP (grade 2, disodium salt; A3377, Sigma–Aldrich), and 0.1 GTP (type 3, disodium salt; G8877, Sigma–Aldrich), pH 7.3 with CsOH). On occasion, the Cs^{+}-based intracellular saline contained 20 mM EGTA, 5 mM $MgCl_2$, and a free Ca^{2+} concentration of 35 nM. In experiments replacing extracellular Ca^{2+} with Ba^{2+}, a Ba^{2+}-Cs^{+}-TEA ASW (as per Ca^{2+}-Cs^{+}-TEA, but with 460 mM TEA-Br instead of TEA-Cl and 11 mM $BaCl_2$ instead of $CaCl_2$) was used. The Cs^{+}-based intracellular saline had a junction potential of 20 mV vs Ca^{2+}-Cs^{+}-TEA ASW or Ba^{2+}-Cs^{+}-TEA ASW, which was compensated for offline. Some cases employed normal ASW (nASW; composition as per tcASW, but with glucose and antibiotics omitted) or Ca^{2+}-free ASW (cfASW; composition as per nASW but with the $CaCl_2$ omitted and 0.5 mM added EGTA) and microelectrodes filled with K^{+}-aspartate-based intracellular saline Ca^{2+} (composition in mM: 500 K-aspartate, 70 KCl, 1.25 $MgCl_2$, 10 HEPES, 11 glucose, 10 glutathione, 5 EGTA, 5 ATP, and 0.1 GTP; pH 7.3 with KOH; free Ca^{2+} concentration set to 300 nM). This intracellular saline had a junction potential of 15 mV vs nASW or cfASW, which was again compensated off-line. Ca^{2+} concentrations were calculated using WebMaxC (http://www.stanford.edu/~cpatton/webmaxcS.htm).

Capacitance tracking

As an indicator of secretion, membrane capacitance was tracked on-line under whole-cell voltage-clamp using the time-domain method in Clampex (Gillis, 1995). From a holding potential of −80 mV, pulses of 100-ms duration and 20-mV amplitude were delivered at 0.5–2 Hz. The voltage step evoked typical, voltage-independent current responses, consisting of a fast transient component (reflecting capacitive current) followed by a steady-state component (reflecting membrane current). The change in current (ΔI) to the 20-mV step (ΔV) was calculated as the difference between the steady-state current (I_{ss}) near the end of the step and the baseline current (I_b) prior to the step: $\Delta I = I_{ss} - I_b$. The membrane time constant (τ) was derived by fitting a single-exponential to the transient current. The charge during the transient current (Q_{tc}) was determined by integrating the area above I_{ss} for the period of the transient current. A correction factor (Q_{cf}), to account for the settling time during the step, was calculated as: $Q_{cf} = \Delta I \times \tau$. The total charge ($Q_t$) was then determined by: $Q_t = Q_{tc} + Q_{cf}$. The total resistance (R_t) was calculated as: $R_t = \Delta V/\Delta I$, while access resistance (R_a) was derived from: $R_a = \tau \times \Delta V/Q_t$. These were used to calculate membrane resistance (R_m) as: $R_m = R_t - R_a$. Finally, membrane capacitance (C_m) was determined from: $C_m = Q_t \times R_t/\Delta V \times R_m$. To increase the accuracy and improve the signal-to-noise ratio, current traces were cumulatively averaged (5–10 pulses per average) before each calculation. The −80 mV holding potential was chosen to avoid the activation of any voltage-gated Ca^{2+} channels during the 20-mV step (Tam et al., 2009).

Double-stranded RNA inhibition

To examine the impact of a reduction in ELH content on secretion, ELH protein expression was lowered with long double-stranded ribonucleic acid (dsRNA) inhibition (Fire et al., 1998; Bhargava et al., 2004). Cultured bag cell neurons were prepared as per Experimental Procedures, Animals and cell culture, with the exception that neurons were plated onto glass coverslips (#1; 48366045; VWR, West Chester, PA, USA) coated with 20 μg/ml poly-L-lysine hydrobromide, MW = 300,000 (P1524-25MG; Sigma–Aldrich) and glued with Sylgard 184 silicone elastomer (SYLG184; World Precision Instruments) to holes drilled out of the bottom of the tissue culture dish.

Abdominal ganglia were dissected from *Aplysia* and the bag cell neuron clusters removed. Clusters were snap-frozen in liquid N_2 and then homogenized in lysis solution from a Norgen Total RNA isolation kit (17200; Norgen Biotek Corp., Thorold, ON, Canada) using a PowerGen 35 handheld homogenizer (Fisher Scientific). Total RNA was isolated and purified using the Norgen kit and analyzed for purity with a spectrophotometer (NanoVue; GE Healthcare Bio-Sciences, Baie d'Urfe, QC, Canada). cDNA was synthesized by reverse transcription using a mixture of poly-A and random hexamer primers and an iScript cDNA synthesis kit (170-8890; Bio-Rad Laboratories, Mississauga, ON, Canada). A 462-bp cDNA fragment encoding *Aplysia* ELH (from accession# NM_001204741.1) was PCR-amplified using an iTaq DNA polymerase kit (170-8870; Bio-Rad Laboratories) and gene-specific primers (forward, 5′-CCACAAAAGGAGACTCCGATTCGACA-3′; reverse, 5′-GAGGTGAGCAGACTGACGCCAGAAC-3′) extended on the 5′ ends with a T7 RNA promoter sequence (TAATACGACTCACTATAGGGAGA). As a negative control, a 450-bp dsRNA was prepared directed against the 5′ untranslated region of the newt (*Notophthalmus viridescens*) retinoic acid receptor (accession# AY847515) using primers (forward, 5′-AGCATGGACCGATCCTAGAG-3′; reverse, 5′-GTTGGGTTCCGTACTGAGGA-3′), again extended on the 5′ ends with a T7 RNA promoter. PCR was performed on 500 ng of the bag cell neuron cluster cDNA, starting with five cycles of melting at 95 °C for 30 s, annealing at 68 °C for 30 s, and elongation at 72 °C for 50 s, followed by 30 cycles of PCR with melting at 95 °C for 30 s, annealing at 72 °C for 30 s, and elongation at 72 °C for 50 s. The PCR product was agarose-gel-purified with an UltraClean GelSpin DNA extraction kit (12400; MO Bio Laboratories Inc., Carlsbad, CA, USA) and used to synthesize sense and antisense cRNA in the same reaction mix with T7 RNA polymerase (4 h at 37 °C) from a MEGAscript RNAi kit (AM1626; Life Technologies, Burlington, ON, Canada). Reactions were treated with DNaseI and RNase (both

from the MEGAscript kit) for 1 h at 37 °C and column purified according to the MEGAscript kit protocol. Bag cell neurons were first cultured in the absence of dsRNA overnight at 14 °C and then bath incubated at 14 °C in the presence of 300 ng/ml dsRNA for an additional 3 d. This method of long dsRNA inhibition has proven successful in both *Aplysia* sensory neurons (Lee et al., 2009) and motor neurons from the related mollusk, *Lymnaea* (Van Kesteren et al., 2006).

Immunocytochemistry

To confirm knock-down, dsRNA-treated neurons were immunostained for ELH at room temperature. The dish was drained of all fluid except for the contents of the glass-bottom well (see Experimental procedures, Double-stranded RNA inhibition) and new solutions delivered by Pasteur pipette directly onto the cells. Neurons were fixed for 25 min with 4% (w/v) paraformaldehyde (04042; Fisher) in 400 mM sucrose/nASW (pH 7.5 with NaOH). They were then permeabilized for 5 min with 0.3% (w/v) Triton X-100 (BP151; Fisher) in fix and washed twice with phosphate-buffered saline (PBS; composition in mM: 137 NaCl, 2.7 KCl, 4.3 Na_2HPO_4, 1.5 KH_2PO_4; pH 7.0 with NaOH). Neurons were blocked for 60 min in a blocking solution of 5% (v/v) goat serum (G9023; Sigma–Aldrich) in PBS. The primary antibody, rabbit anti-ELH immunogammaglobulin (IgG) (kindly provided by Dr. NL Wayne, University of California Los Angeles), was applied at 1:1000 in blocking solution. Neurons were incubated in the dark for 1 h and subsequently washed 4× with PBS. The secondary antibody, goat anti-rabbit IgG conjugated to Alexa Fluor 488 (A-11008; Invitrogen) was applied at 1:200 in blocking solution and incubated in the dark for 2 h. Neurons were then washed 4× with PBS, the wells filled with mounting solution (26% w/v glycerol (BP2291; Fisher), 11% w/v Mowiol 4-88 (17951; Polysciences, Warrington, PA, USA), and 110 mM TRIS (pH 8.5)) and covered with a glass coverslip.

Fluorescence microscopy

Stained neurons were imaged using a Nikon TS100-F inverted microscope (Nikon, Mississauga, ON, Canada) equipped with Nikon Plan Fluor 20× (numerical aperture 0.50) or 100× objective (numerical aperture 1.30). Neurons were excited with a 50-W Mercury lamp and a 480/15 nm band pass filter. Fluorescence was emitted to the eyepiece or camera through a 505-nm dichroic mirror and 520-nm barrier filter. Images (1392 × 1040 pixels) were acquired at the mid-vertical somatic axis focal plane using a Pixelfly USB camera (PCO-TECH, Romulus, MI, USA/Photon Technology International, London, ON, Canada) and the Micro-Manager 1.4.5 plugin (http://valelab.ucsf.edu/~MM/MMwiki/index.php/Micro-Manager) for ImageJ 1.43 (http://rsbweb.nih.gov/ij/) with 20- or 50-ms exposure times.

Reagents and drug application

Carbonyl cyanide 4-(trifluoromethoxy) phenylhydrazone (FCCP; 21857; Sigma–Aldrich), cyclopiazonic acid (CPA; C1530; Sigma–Aldrich or 239805; Calbiochem, San Diego, CA, USA), and bafilomycin A (B1793; Sigma–Aldrich) were made up as stocks in dimethyl sulfoxide (DMSO; BP231; Fisher). N-ethylmaleimide (NEM; E3876; Sigma–Aldrich) was dissolved as a stock in 100% ethanol. The maximal final concentration of either vehicle was $\leqslant$0.2%, which we have found to have no adverse affect on the membrane potential, macroscopic or single-channel currents, membrane capacitance, or intracellular Ca^{2+} of bag cell neurons (Magoski et al., 2000; Kachoei et al., 2006; Lupinsky and Magoski, 2006; Hung and Magoski, 2007; Gardam et al., 2008; Geiger and Magoski, 2008; Tam et al., 2009; Hickey et al., 2010). $NiCl_2$ (N6136; Sigma–Aldrich) and guanosine-5′-[γ-thio]triphosphate (GTP-γ-S; tetralithium salt; G8634; Sigma–Aldrich) were prepared as stocks in water.

Solution exchanges were accomplished by manual perfusion using a calibrated transfer pipette to first exchange the bath (tissue culture dish) solution. To apply a drug, a small volume (1–10 μl) of stock solution was mixed with a larger volume of saline (approximately 100 μl) that was initially removed from the bath, and this mixture was then pipetted back into the bath. Care was taken to add drugs near the side of the dish and as far away as possible from the neurons. GTP-γ-S was diluted down in intracellular saline and dialyzed directly into the neuron via the whole-cell recording pipette.

Analysis

Clampfit, a program of pClamp, was used to quantify membrane capacitance. Typically, the analysis involved comparing the average value during a steady-state baseline of 30 s to 1 min, with either the peak response following a train of depolarizing stimuli (see Results for details) or the average peak value from a region that had reached steady-state for 5–30 s after the delivery of a drug (again see Results for details). Average values were determined by eye or by setting cursors on either side of the range of interest and calculating the mean score of those data points. Change was expressed as a percent change of the new capacitance over the baseline capacitance. The time course of the response was quantified by determining the percent recovery from the peak change in capacitance back down to baseline over a period of 5 or 10 min. In some instances, Ca^{2+} current during a train of step depolarizations was recorded. To estimate total Ca^{2+} influx, the area above each current trace was calculated in Clampfit between cursors set at the start and end of the trace, divided by whole-cell capacitance, and summed with the values derived from all other traces in a given neuron.

The staining intensity of fluorescence images was quantified as the average intensity, in arbitrary units, using ImageJ and a free-hand drawn circle region of interest over the soma to best fit the outline of the apparent edge of the membrane. Intensity was then normalized by dividing all values within a given cohort of neurons by the maximally fluorescing cell.

Summary data are presented as the mean ± standard error of the mean. Statistics were

performed using Instat (version 3.0; GraphPad Software, San Diego, CA, USA). The Kolmogorov–Smirnov method was used to test data sets for normality. If the data were normal, Student's unpaired *t*-test (for normally distributed data) with the Welch correction as necessary (for unequal standard deviations) was used. A Mann–Whitney test was implemented if the data were not normal. To test for differences between multiple means, a standard one-way analysis of variance (ANOVA) was used, followed by Bonferroni's multiple comparisons test. Means were considered significantly different if the *p*-value was <0.05.

RESULTS

Ca^{2+} entry causes an increase in bag cell neuron membrane capacitance

It is well established that capacitance tracking can reflect secretion, based on vesicle fusion causing an increase in membrane surface area (Neher and Marty, 1982; Lim et al., 1990; Klyachko and Jackson, 2002). Furthermore, Geiger and Magoski (2008) reported that delivery of a stimulus which mimics the fast phase of the afterdischarge (a 5-Hz, 1-min burst of action potentials) evokes an immediate and prominent influx of Ca^{2+} through bag cell neuron voltage-gated Ca^{2+} channels. To investigate if Ca^{2+} influx could trigger secretion, the membrane capacitance of individual, cultured bag cell neurons was tracked under voltage-clamp while emulating the fast phase with a 5-Hz, 1-min train of 75-ms square voltage pulses from −80 mV to 0 mV. In solutions that isolate Ca^{2+} currents (Ca^{2+}-Cs^{+}-TEA ASW external and Cs^{+}-aspartate internal) (Fig. 1A, inset), the train caused a robust capacitance increase that decayed to baseline over 5–10 min ($n = 8$) (Fig. 1A, upper).

The vast majority of neurons used in the present study had sprouted neurites. However, because the presence of neurites and growth cones may be necessary for peptide release, we initially noted neuronal shape and size during recordings so to ascertain any potential correlation in secretory capability. The train-induced capacitance elevation was apparent in cultured bag cell neurons regardless of whether or not they had sprouted and were essentially spherical ($n = 2$), had extended one or more short neurites (less than one soma diameter) ($n = 4$), or had extended one or more long neurites (greater than one soma diameter) ($n = 9$). In addition, to certify that the protease used to prepare the neurons for isolation did not impact secretion, neurons were cultured without prior enzymatic treatment. Not surprisingly, isolation without protease resulted in a very low yield ($n = 3$ neurons from two animals); yet those cells, which also did not sprout, still presented a similar capacitance elevation (9.8 ± 2.1%; $n = 3$) compared to additional controls (9.7 ± 2.4%; $n = 8$) cultured using protease.

Ba^{2+} is commonly used as a substitute for Ca^{2+} because it readily passes through Ca^{2+} channels (Hagiwara et al., 1974; Hille, 2001); for example, both our laboratory and others have found that Ca^{2+} currents recorded in Ba^{2+} are as large, if not larger, than those measured using Ca^{2+} (Fieber, 1995; Knox et al., 1996; Tam et al., 2009). However, Ca^{2+} is often specifically required to initiate processes such as channel gating or secretion (Miledi, 1966; Shin et al., 2003; Lupinsky and Magoski, 2006). When extracellular Ca^{2+} was replaced with Ba^{2+} by using Ba^{2+}-Cs^{+}-TEA ASW rather than Ca^{2+}-Cs^{+}-TEA ASW, it abolished the rise in membrane capacitance produced by the train ($n = 11$) (Fig. 1A, lower). This reduction in the capacitance change was significant (Fig. 1B).

Compared to the secretion of classical transmitters, release from neuroendocrine cells is often slower to develop and requires greater Ca^{2+} entry, i.e., higher frequency or longer bouts of firing (Neher, 1998; Neher and Sakaba, 2008). To determine if there was an optimal level of stimulation for generating a membrane capacitance change, neurons were voltage-clamped at −80 mV and stepped to 0 mV with a 5-Hz, 1-min train of 10-, 25-, 37-, 50-, 75-, or 100-ms square voltage pulses. Only one train with a given pulse duration, chosen at random, was applied to an individual neuron. While essentially no response occurred at 10 or 25 ms, a small capacitance elevation was apparent with 37 ms, and this was even larger for 50 ms, but did not increase further at 75 or 100 ms (Fig. 1C). For consistency, and given that, on the whole, it represents the middle of the most effective range for evoking the response, a 75-ms pulse duration was chosen for all subsequent experiments involving the train.

To examine how Ca^{2+} influx related to the capacitance increase, Ca^{2+} currents were recorded from separate cultured bag cell neurons using the train and the full range of pulse durations (e.g., Fig. 1A, inset). Influx was calculated by summing the area above each current pulse and normalized to cell capacitance (see Experimental procedures, Whole-cell voltage-clamp recording for details). Ca^{2+} influx was evident even at a pulse duration of 10 ms (albeit small), and steadily increased as the pulses were lengthened, with a half-maximum near 37 ms and a plateau by 50 ms (Fig. 1D). Thus, when comparing Fig. 1C vs D, the capacitance change is not apparent until the Ca^{2+} influx has surpassed half of the upper limit.

A general Ca^{2+} channel blocker eliminates the increase in capacitance

To further test whether Ca^{2+} entry through voltage-gated Ca^{2+} channels is responsible for secretion, we applied the common Ca^{2+} channel blocker, Ni^{2+}, before delivering the train (Byerly et al., 1985; McFarlane and Gilly, 1998). Specifically, cultured bag cell neurons bathed in Ca^{2+}-Cs^{+}-TEA ASW and dialyzed with Cs^{+}-based intracellular saline, were subjected to consecutive 5-Hz, 1-min trains separated by approximately 15 min ($n = 10$). The purpose of administering two trains was to first confirm that an individual neuron was capable of responding before attempting to block Ca^{2+} influx. Both trains elicited a rise in membrane capacitance, although the second increase was always smaller than the first by essentially 50% (Fig. 2A). When 10 mM Ni^{2+} was

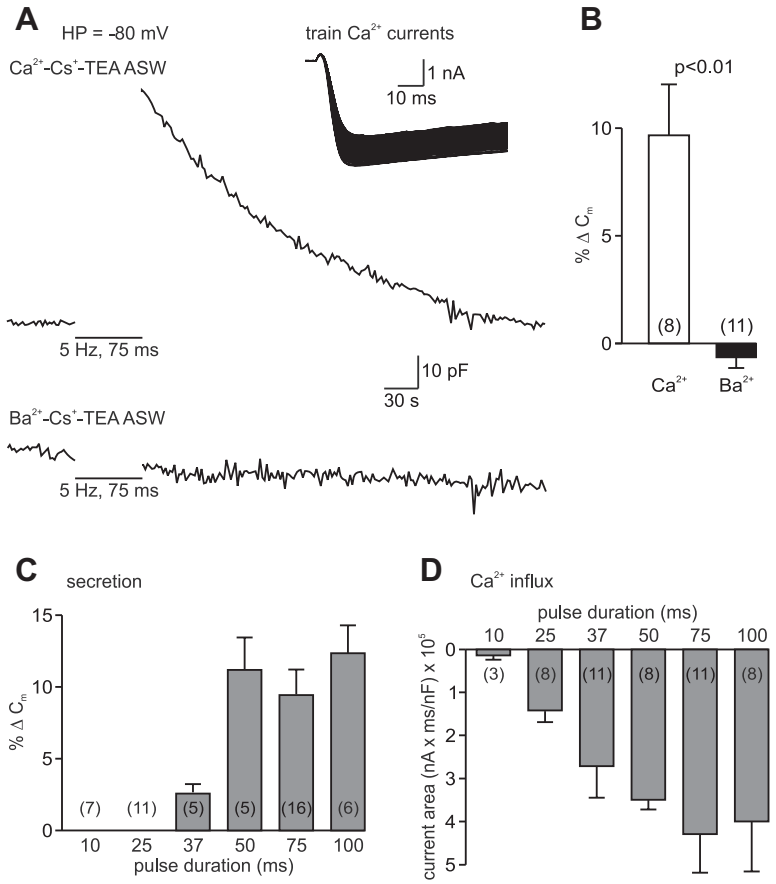

Fig. 1. Ca^{2+} influx initiates an increase in the membrane capacitance of bag cell neurons. (A) Upper trace, cultured bag cell neurons are whole-cell voltage-clamped at a holding potential (HP) of −80 mV using solutions to isolate Ca^{2+} currents (Ca^{2+}-Cs^{+}-TEA ASW external and Cs^{+}-aspartate-based intracellular saline internal). Membrane capacitance is tracked with the time domain technique. A 5-Hz, 1-min train of 75-ms pulses from −80 mV to 0 mV causes a rapid, transient elevation in capacitance. Lower trace, this effect is eliminated in a different neuron when Ca^{2+} in the external solution is replaced with Ba^{2+} (Ba^{2+}-Cs^{+}-TEA ASW). Scale bars apply to both traces. The gap during the train is due to the tracking software being incompatible with the large change in membrane conductance produced by the depolarization. Inset, an example of Ca^{2+} currents during the 5-Hz, 1-min train. All 300 traces are superimposed. (B) Summary data comparing the mean percent change in capacitance following the train show a significant difference when external Ca^{2+} is substituted with Ba^{2+} (two-tailed unpaired *t*-test, Welch corrected). The percent change in capacitance reflects the peak change normalized to baseline. For this and subsequent bar graphs, data represent the mean ± standard error of the mean, with the n value indicated in or above the bars. (C) Summary data of the mean percent change in capacitance following a train with pulse durations of 10 though to 100 ms. Essentially no change occurs with the 10- or 25-ms pulse duration, and only with a 37-ms pulse is an elevation in capacitance first seen. Subsequently, a more prominent response is apparent with 50-, 75-, and 100-ms pulse durations, although there is no difference between the magnitude of the change produced by these stimuli. (D) Mean data of Ca^{2+} influx as reflected by the sum of the current area during all sweeps evoked by the train over a range of pulse durations (different neurons from C). The current area is normalized for cell size by dividing by the neuronal capacitance. A small amount of total influx is observed with the 10-ms pulse duration, which grows steadily for the 25- and 37-ms pulses, and plateaus by the 50-ms pulse duration.

delivered prior to the second train, it completely eliminated the subsequent change in capacitance (Fig. 2B), which reached significance in the group data (n = 5) (Fig. 2C). Previous work in our laboratory has shown 10 mM Ni^{2+} to be saturating for Ca^{2+} channel block in bag cell neurons (Hung and Magoski, 2007). We also tested if the train-induced capacitance increase was maintained under the more physiological conditions of a simple culture medium in the bath and K^{+}-based intracellular saline in the pipette. In this case, the response was still present and significantly reduced by Ni^{2+} (Fig. 2D). In both conditions, we did observe some cases where stimulation in Ni^{2+} lead to subsequent decreases in capacitance, which could be due to voltage-dependent activation of endocytosis – as seen in dorsal root ganglion neurons (Zhang et al., 2004).

Buffering intracellular Ca^{2+} attenuates the increase in membrane capacitance

There appears to be a strong link between Ca^{2+} entry and the capacitance response. To determine whether the train-induced increase in capacitance required an elevation of intracellular Ca^{2+}, cultured bag cell neurons were bathed in Ca^{2+}-Cs^{+}-TEA ASW and dialysed for 10 min with Cs^{+}-based intracellular solution containing either our standard (5 mM) or a high (20 mM) concentration of the slow Ca^{2+} buffer, EGTA (Smith et al., 1984; Naraghi, 1997). When intracellular Ca^{2+}

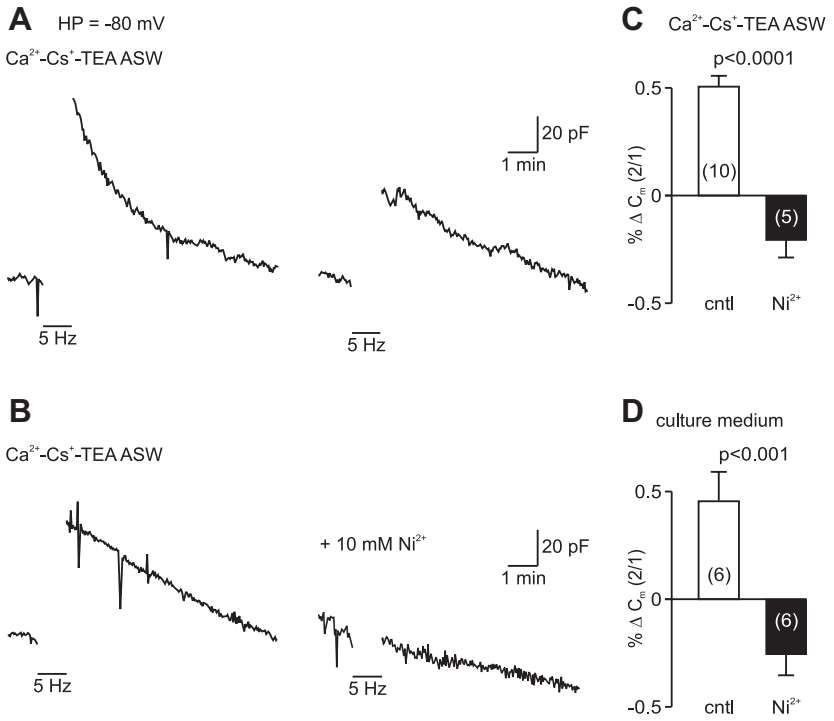

Fig. 2. Ni^{2+} blocks the increase in membrane capacitance. (A) Two consecutive 5-Hz, 1-min trains delivered to a single neuron 14 min apart while tracking capacitance under whole-cell voltage-clamp at −80 mV. The neuron is bathed in Ca^{2+}-Cs^{+}-TEA ASW and dialyzed with Cs^{+}-based intracellular saline. Both trains produce a change in capacitance, but the second elevation is consistently smaller than the first. Scale bars apply to both traces. (B) In a separate neuron, the addition of 10 mM Ni^{2+}, a common Ca^{2+} channel blocker, prior to the second train eliminates the change in capacitance. Again, scale bars apply to both traces. (C) Summary data of the second response over the first indicate that the second train is about half as effective at eliciting a capacitance change as the first train. Moreover, there is no change in capacitance with the second train in Ni^{2+} (one-tailed unpaired *t*-test). (D) Summary data as per above, but with culture medium as the external solution, also demonstrate a near 50% rundown in the capacitance change brought about by the second train. Ni^{2+} also prevents the effect of the train on membrane capacitance (one-tailed unpaired *t*-test).

was buffered with high-EGTA (n = 10), the rise in membrane capacitance caused by the 5-Hz, 1-min train was attenuated by nearly half compared to the response evoked under the lower concentration of EGTA (n = 9) (Fig. 3A). This effect achieved significance (Fig. 3B) and suggests the change in membrane capacitance is dependent on elevated intracellular Ca^{2+}.

An alkylating agent inhibits the increase in membrane capacitance

Blocking one of the steps leading to vesicle-plasma membrane fusion should reduce the capacitance increase evoked by the train. N-ethylmaleimide (NEM) is an alkylating agent that disrupts protein sulfhydryl groups and can block vesicle fusion (Block et al., 1988; Han et al., 1999; Wickner and Schekman, 2008). We treated cultured bag cell neurons for 30 min with either ethanol (the vehicle) or 100 μM NEM, and subsequently delivered a 5-Hz, 1-min train under whole-cell voltage-clamp in Ca^{2+}-Cs^{+}-TEA ASW using with Cs^{+}-based intracellular solution. Following NEM exposure (n = 5), the train produced an increase in capacitance that was diminished by two-thirds compared with ethanol-treated neurons (n = 5) (Fig. 4A). The mean data showed this reduction met the level of significance (Fig. 4B). This aside, NEM could modify other sulfhydryl-containing proteins; in fact, NEM may indirectly modulate Ca^{2+} currents in some neurons, via alkylation of cysteine residues on G-protein subunits (Fryer, 1992; Shapiro et al., 1994). To rule out the possibility that NEM impacted Ca^{2+} influx, peak Ca^{2+} currents were measured from a holding potential of −60 mV using 200-ms, 10-mV incremental depolarizations to +40 mV after a 30-min treatment of either ethanol (n = 6) or 100 μM NEM (n = 7) (Fig. 4C). The resulting current–voltage relationships were essentially identical between the two conditions (Fig. 4D). In addition, separate experiments showed there was no significant difference between the total peak Ca^{2+} current during a train following ethanol (−658.0 ± 111.1 nA/nF; n = 5) vs NEM (−381.2 ± 85.8 nA/nF; n = 5) ($p > 0.05$, two-tailed unpaired *t*-test).

dsRNA inhibition of ELH reduces peptide expression and the change in membrane capacitance

If the train-induced increase in capacitance is due to peptide secretion, then a reduction in bag cell neuron peptide content should decrease the response. To achieve this, cultured bag cell neurons were incubated for 3 d in 300 ng/ml dsRNA targeting the *Aplysia* ELH precursor mRNA, which codes for both the 36 amino acid ELH peptide itself and the three pentapeptides,

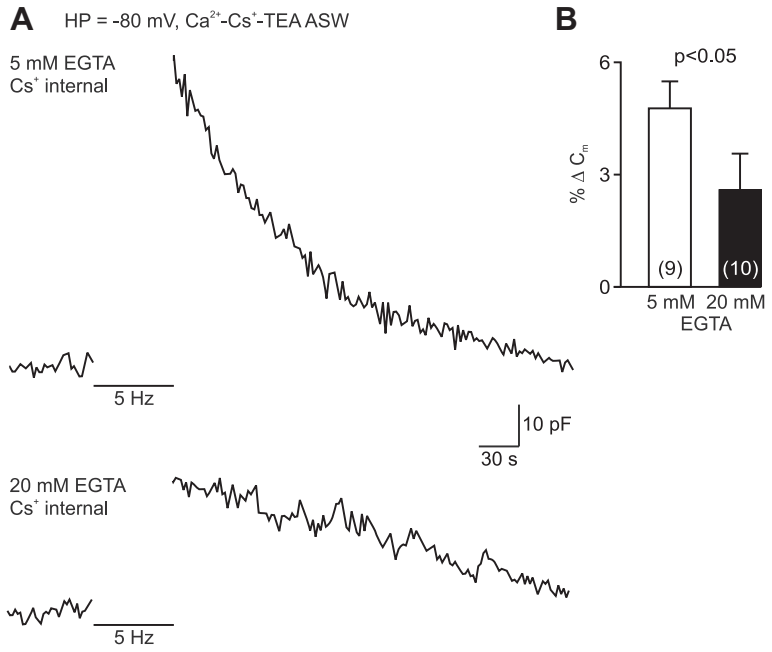

Fig. 3. High concentrations of intracellular EGTA reduce the increase in membrane capacitance. (A) Capacitance tracking of two different neurons whole-cell voltage-clamped at −80 mV in Ca^{2+}-Cs^{+}-TEA ASW and dialyzed for 10 min with either our standard Cs^{+}-based intracellular saline or saline supplemented with high-EGTA. In comparison with control intracellular saline (5 mM EGTA, upper trace), the rise in membrane capacitance following delivery of a 5-Hz, 1-min train is markedly reduced when intracellular Ca^{2+} is buffered by high-EGTA (20 mM, lower trace). Scale bars apply to both traces. (B) Summary data of the mean percent change in membrane capacitance show that the increase induced by the train is significantly less when 5 mM ETGA intracellular saline is substituted with 20 mM EGTA intracellular saline (one-tailed unpaired *t*-test).

α-, β-, and γ-bag cell peptide (Scheller et al., 1983; Newcomb et al., 1988; Sossin et al., 1990; Fire et al., 1998). These are the reproductively-active components secreted from bag cell neurons during the afterdischarge (Loechner et al., 1990, 1992; Hatcher and Sweedler, 2008). The control consisted of incubating sister bag cell neuron cultures in 300 ng/ml dsRNA of the newt retinoic acid receptor 5′ untranslated region. A comparison of the newt sequence with both the *Aplysia* genome and transcriptome found no significant similarity. Reductions in ELH content were verified by immunocytochemically staining cultured bag cell neurons using rabbit anti-ELH primary antibody followed by goat anti-rabbit Alexa Fluor 488 secondary antibody (see below). Prior immunocytochemistry, immunohistochemistry, immunoblotting, and radio-immunoassay have demonstrated that the primary antibody specifically recognizes ELH in *Aplysia* nervous tissue, including the bag cell neurons *in situ* and *in vitro*, as well as ELH secreted into the hemolymph (Newcomb et al., 1988; Jonas et al., 1997; White and Kaczmarek, 1997; Wayne et al., 1998; Michel and Wayne, 2002).

ELH staining of cultured bag cell neurons required the presence of both antibodies, with essentially no fluorescence signal detected following incubation in the secondary antibody alone (n = 12; data not shown). However, application of the primary and secondary antibody in series produced robust staining of control-treated neurons (n = 24) (Fig. 5A, left). As per previous reports (Chiu and Stumwasser, 1981; White and Kaczmarek, 1997), ELH staining was observed throughout cultured bag cell neurons, with the signal from the soma being more intense vs the neurites and growth cones. Staining was substantially less when bag cell neurons were treated with ELH dsRNA (n = 18) (Fig. 5A, right). Quantification of the somatic signal revealed a significant reduction, by about half, in the fluorescence intensity for ELH dsRNA compared to control (Fig. 5C). Closer examination of 13 growth cones revealed a reduction in overall staining intensity and the number of puncta in ELH dsRNA-treated neurons as opposed to control (Fig. 5B).

The impact of ELH knock-down on secretion was tested with capacitance tracking by voltage-clamping bag cell neurons at −80 mV using Ca^{2+}-Cs^{+}-TEA ASW and the Cs^{+}-based intracellular solution. Control neurons presented a robust increase in membrane capacitance following the 5-Hz, 1-min train (n = 11) (Fig. 5D, left). Conversely, the response of neurons incubated in ELH dsRNA was nearly halved (n = 10) (Fig. 5D, right). The difference between control and ELH dsRNA in the grouped data proved significant (Fig. 5E).

Depletion of Ca^{2+} from mitochondria, but not endoplasmic reticulum, elevates membrane capacitance

Along with voltage-gated Ca^{2+} influx, intracellular Ca^{2+} may also be liberated from either the mitochondria or the endoplasmic reticulum (Knox et al., 1996; Jonas et al., 1997; Kachoei et al., 2006; Geiger and Magoski, 2008; Gardam et al., 2008). To examine the potential for these stores to trigger secretion, organelles were depleted of Ca^{2+} while tracking the capacitance of

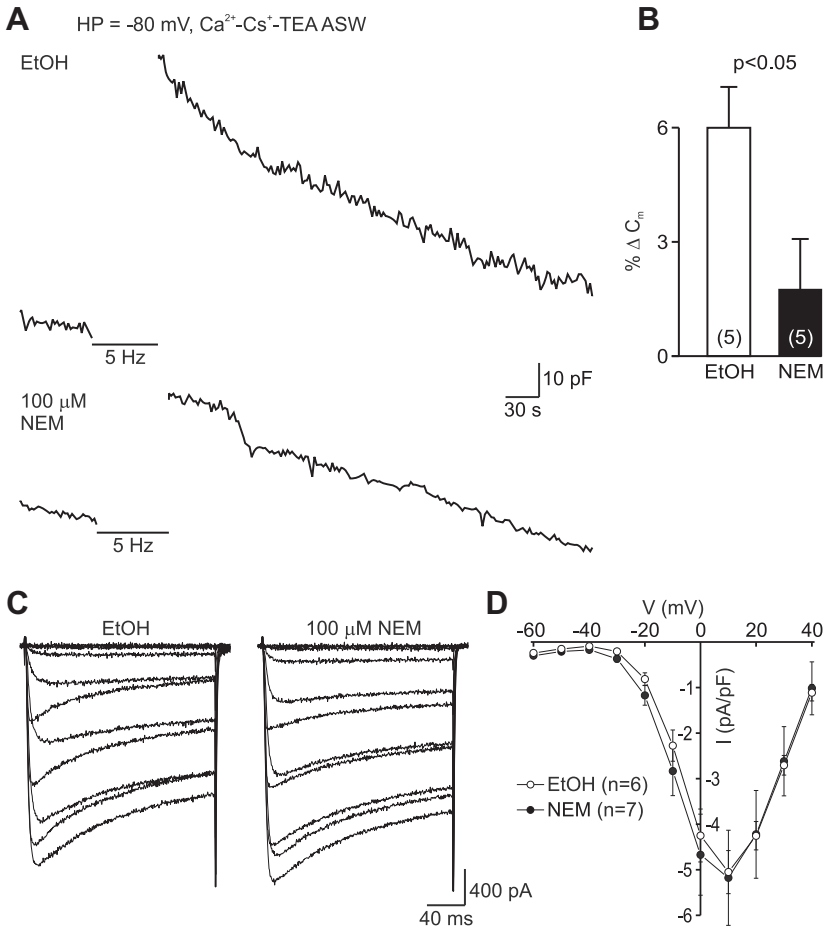

Fig. 4. N-ethylmaleimide inhibits the increase in membrane capacitance. (A) Separate neurons under whole-cell voltage-clamp at −80 mV while tracking capacitance in Ca^{2+}-Cs^{+}-TEA ASW with Cs^{+}-based intracellular saline. Prior to the delivery of a 5-Hz, 1-min train, the cells were treated for 30 min with either ethanol (EtOH; the vehicle) or 100 μM NEM. The elevation in membrane capacitance evoked by the train is diminished after treatment with NEM (lower trace) vs treatment with ethanol (upper trace). Scale bars apply to both traces. (B) Summary data show a significant reduction in the mean percent increase in capacitance evoked by the 5 Hz, 1-min train following NEM as opposed to incubation in ethanol (two-tailed unpaired *t*-test). (C) Ca^{2+} currents from different neurons elicited with 200-ms square pulses from −60 mV in 10-mV increments to +40 mV. The currents observed after 30 min of ethanol (left traces) are very similar to those in 100 μM NEM (right traces) for the same time period. Scale bars apply to both traces. (D) Summary data showing peak Ca^{2+} current normalized to capacitance and plotted against step voltage. There is no difference in the current following pretreatment with NEM (closed circles) vs ethanol (open circles).

cultured bag cell neurons dialyzed with K^{+}-aspartate-based intracellular saline under whole-cell voltage-clamp at −80 mV in nASW. FCCP is a protonophore that collapses the mitochondrial membrane potential and allows Ca^{2+} to leak out of the organelle into the cytosol (Heytler and Prichard, 1962; Simpson and Russell, 1996; Babcock et al., 1997). In response to 20 μM FCCP (n = 11), a relatively slow-onset elevation in membrane capacitance was observed (Fig. 6A, upper trace). This response was typically smaller than the capacitance change produced by the train. We also investigated whether releasing endoplasmic reticulum Ca^{2+} with CPA, a Ca^{2+}-ATPase blocker (Seidler et al., 1989), was capable of stimulating secretion. Unlike FCCP, 20 μM CPA (n = 6) did not cause an increase in membrane capacitance (Fig. 6A, lower trace), and the difference between the two reagents reached the level of significance (Fig. 6B).

Vesicles and lysosomes, known as the acidic store, use a V-type H^{+}-ATPase to maintain negative pH, which is then harnessed to sequester Ca^{2+} via H^{+}/Ca^{2+} exchange (Goncalves et al., 1999; Christensen et al., 2002). The protonophore action of FCCP could collapse the acidic store H^{+} gradient and cause secretion by freeing up non-mitochondrial Ca^{2+} (Han et al., 1999) To rule this out, neurons were exposed to 100 nM of the H^{+}-ATPase inhibitor, bafilomycin A (Bowman et al., 1988), which we have shown liberates non-mitochondrial/non-endoplasmic reticulum Ca^{2+} (Kachoei et al., 2006; Hickey et al., 2010). However, bafilomycin A did not significantly increase membrane capacitance (n = 6) (Fig. 6B).

The mitochondrial Ca^{2+} released by FCCP could activate one of the several Ca^{2+}-dependent and Ca^{2+}-permeable non-selective cation channels in bag cell neurons (Lupinsky and Magoski, 2006; Gardam et al., 2008; Geiger et al., 2009; Hickey et al., 2010). This Ca^{2+} entry could induce secretion separate from that evoked by mitochondrial Ca^{2+} itself. To distinguish between Ca^{2+} influx and Ca^{2+} release, cultured bag

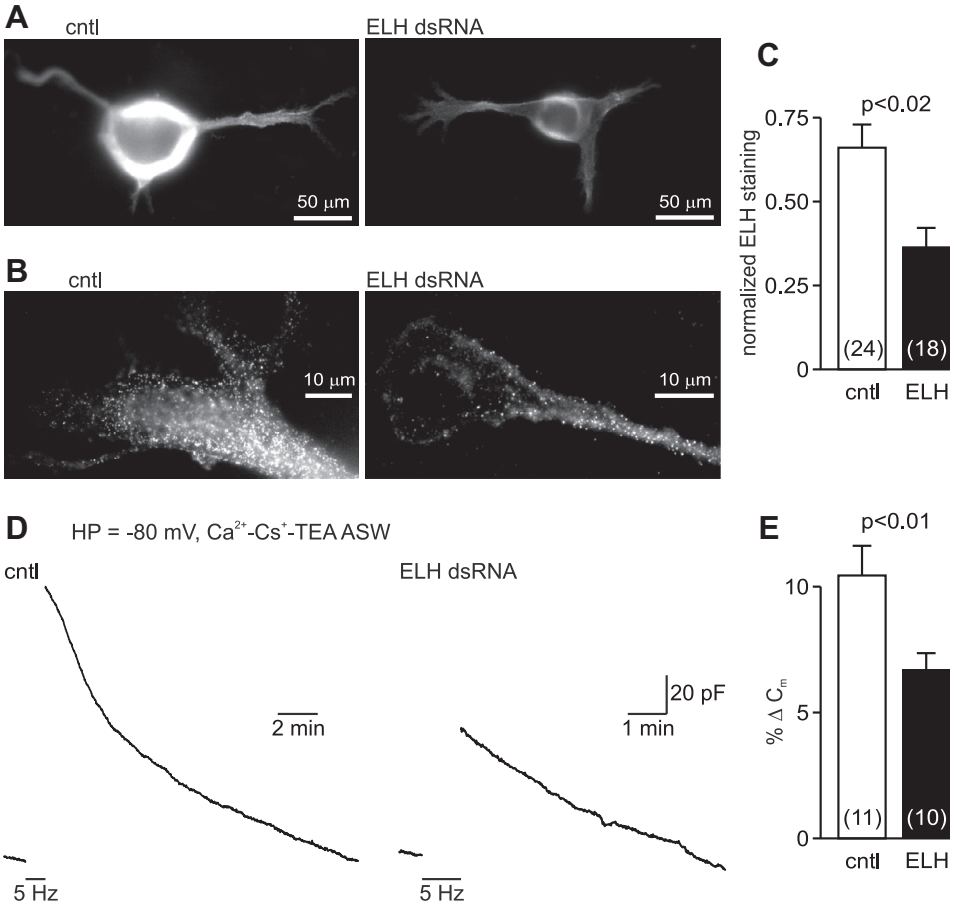

Fig. 5. dsRNA inhibition of ELH expression attenuates the increase in membrane capacitance. (A) Cultured bag cell neurons immunostained for ELH (1:1000 rabbit anti-ELH IgG followed by 1:200 goat anti-rabbit IgG - Alexa Fluor 488). Left panel, a control neuron (incubated in 300 ng/ml dsRNA corresponding to the 5′ untranslated region of the newt retinoic acid receptor) shows intense staining in the soma as well as the two, primary neurites. Right panel, a separate neuron from the same culture group, but exposed to 300 ng/ml ELH dsRNA, has far less signal throughout the soma and the three primary neurites. (B) ELH immunostained growth cones from two, separate bag cell neurons (different from those shown in A). Left panel, under control conditions there is marked staining both in the end of the neurite (lower right portion of photomicrograph) and growth cone central domain, and as well as a high density of punctate staining in the lamellar and filopodial areas. Right panel, in a growth cone from a different neuron, treated with ELH dsRNA, the overall signal and the quantity of puncta are considerably reduced throughout the neurite end, central domain, and lamellipodia. (C) Summary data of somatic ELH immunostaining reveal that exposure to ELH dsRNA results in a significant, near 50% reduction in signal compared to control (one-tailed Mann–Whitney test). (D) Exposure to ELH dsRNA lessens the train-induced capacitance elevation. Left, a cultured bag cell neuron incubated in 300 ng/ml newt retinoic acid receptor dsRNA displays a robust increase in membrane capacitance following a 5-Hz, 1-min train applied under voltage-clamp at −80 mV in Ca^{2+}-Cs^{+}-TEA ASW with Cs^{+}-based intracellular saline. Right, capacitance tracking from another neuron, which has been subjected to 300 ng/ml ELH dsRNA, presents a reduced train-evoked response. The ordinate scale bar applies to both traces. (E) A comparison of the group data indicates that there is a significant difference in the ELH dsRNA- vs the control (newt dsRNA)-treated neurons (one-tailed unpaired *t*-test).

cell neurons were voltage-clamped at −80 mV using the K^{+}-based intracellular saline and bathed in either nASW (11 mM Ca^{2+}) or cfASW (0 Ca^{2+}, 0.5 mM EGTA), while administering 20 μM FCCP. There was no significant difference between the rise in membrane capacitance provoked by FCCP in nASW (n = 7) vs cfASW (n = 9) (Fig. 6C, D), implying that mitochondrial Ca^{2+} directly causes secretion.

To confirm the possibility that secretion is elicited by mitochondrial Ca^{2+}, experiments involving buffering of intracellular Ca^{2+}, similar to those performed for the train-induced capacitance rise, were undertaken. Specifically, cultured bag cell neurons were bathed in nASW and dialysed for 30 min with Cs^{+}-based intracellular solution including either 5 mM EGTA (as control) or 20 mM EGTA (to strongly buffer Ca^{2+}). Compared to control (n = 4), introducing a high concentration of EGTA (n = 5) into the neurons lessened the elevation of membrane capacitance due to 20 μM FCCP by about two-thirds (Fig. 6E), which met the level of significance (Fig. 6F).

The pools released by mitochondrial Ca^{2+} and Ca^{2+} influx overlap

As is the case for classical neurotransmission, the secretion of neuropeptides is thought to originate from a readily releasable pool of vesicles (Burke et al., 1997; Barg et al., 2002). To establish if voltage-gated Ca^{2+} influx and mitochondrial Ca^{2+} access the same or different pools of releasable vesicles, cultured bag cell neurons were pretreated for 10–20 min with vehicle or

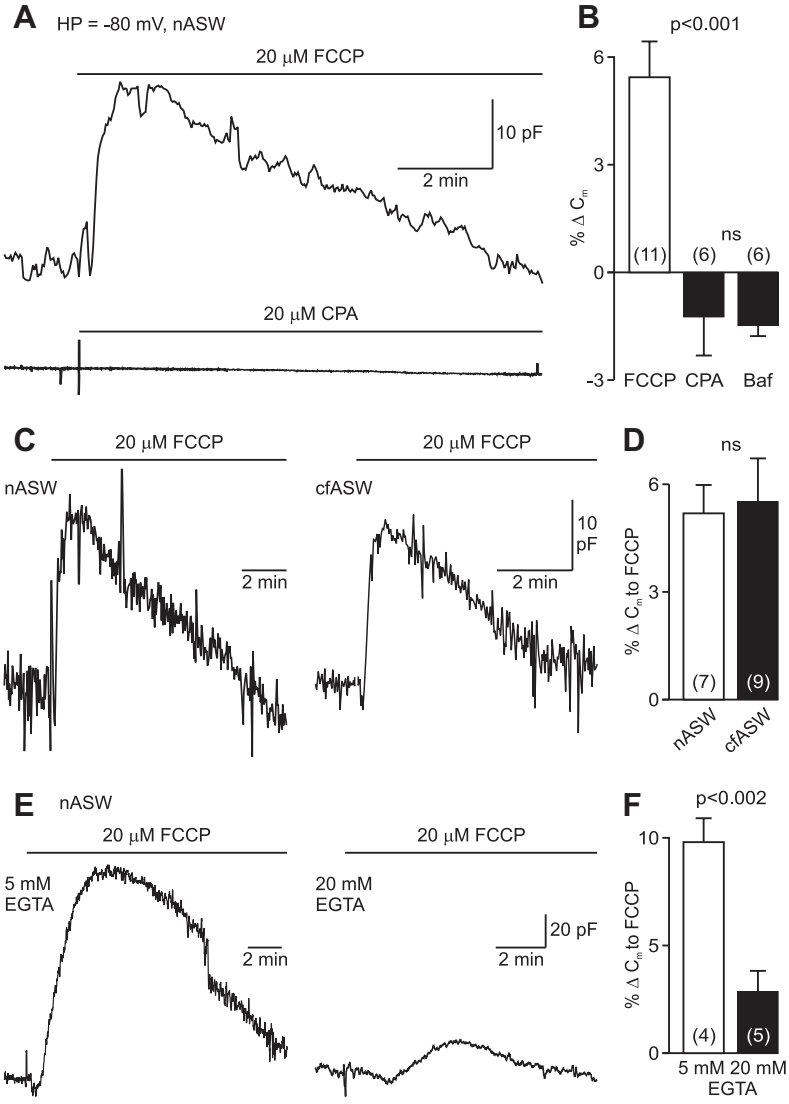

Fig. 6. Depletion of mitochondrial Ca^{2+} causes an increase in membrane capacitance. (A) Upper trace, capacitance tracking under whole-cell voltage-clamp at −80 mV in nASW with K^+-aspartate-based intracellular saline. Depleting mitochondrial Ca^{2+} stores by collapsing organelle membrane potential with 20 μM FCCP results in a transient elevation in membrane area. Lower trace, in a different neuron, depleting endoplasmic reticulum Ca^{2+} stores with 20 μM of the Ca^{2+}-ATPase blocker, CPA, does not change capacitance. The artifact at the beginning of the trace is due to the addition of the drug. Scale bars apply to both traces.(B) Summary data show a significant difference between the mean percent change in membrane capacitance due to FCCP and CPA or 100 nM bafilomycin A (Baf) (ANOVA, Bonferroni's multiple comparisons test). (C) Two individual neurons whole-cell voltage-clamped at −80 mV. The change in capacitance following FCCP is essentially the same when the cell is bathed in Ca^{2+}-containing nASW (left trace) or without external Ca^{2+} in cfASW (right trace). The ordinate scale bar applies to both traces. (D) Summary data show that the mean percent increase in membrane capacitance provoked by FCCP is not significantly different between nASW and cfASW (two-tailed unpaired *t*-test). (E) Separate neurons bathed in nASW and held at −80 mV under whole-cell voltage-clamp. For a cell dialysed for 30 min with Cs^+-based intracellular saline containing 5 mM EGTA (left trace), the addition of FCCP results in a clear capacitance rise. However, the FCCP response is clearly smaller when 20 mM EGTA buffers the intracellular Ca^{2+} (right trace). The ordinate scale bar applies to both traces. (F) Group data reveal a significant drop in the average FCCP-induced percent change in membrane capacitance subsequent to dialysis with 20 mM EGTA vs 5 mM ETGA intracellular saline (one-tailed unpaired *t*-test).

20 μM FCCP in order to deplete mitochondrial Ca^{2+} and cause some secretion. Neurons were pretreated, rather than applying both FCCP and the train after establishing recording, because it proved difficult to hold the cells long enough to carry out both procedures, particularly after eliminating mitochondrial function. Subsequently, the 5-Hz, 1-min train was delivered under voltage-clamp at −80 mV in Ca^{2+}-Cs^+-TEA ASW with Cs^+-based intracellular saline while tracking membrane capacitance. The capacitance increase following the train was around two-thirds smaller in neurons which saw FCCP (n = 6) relative to control (n = 7) (Fig. 7A). The group data demonstrated that this difference was significant (Fig. 7B).

A non-hydrolyzable guanosine nucleotide impacts the FCCP-induced, but not train-induced, change in capacitance

If the increase in membrane capacitance represents exocytosis, the complement would be that the recovery of capacitance toward baseline represents endocytosis

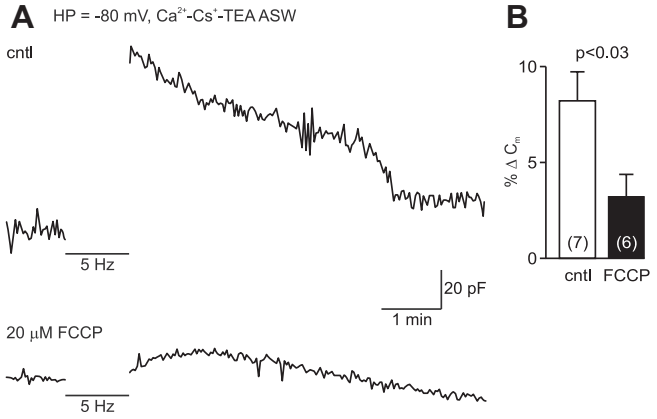

Fig. 7. The capacitance increase brought about by voltage-gated Ca^{2+} influx is reduced following mitochondrial Ca^{2+} depletion. (A) Records of capacitance tracking from two individual neurons under whole-cell voltage-clamp at −80 mV in Ca^{2+}-Cs^{+}-TEA ASW with Cs^{+}-based intracellular saline. Prior depletion of mitochondrial Ca^{2+} stores with a 10-min pretreatment in 20 μM FCCP (lower trace) attenuates the capacitance increase following a 5-Hz, 1-min train compared to control (upper trace). Scale bars apply to both traces. (B) Summary data comparing the mean percent change in train-induced elevation in membrane capacitance in control and FCCP-treated neurons indicate a significant difference (two-tailed unpaired *t*-test).

(Smith et al., 2008). Classical membrane retrieval occurs via clathrin-coated pits that are pinched off by the GTPase, dynamin (Van Der Bliek and Meyerowitz, 1991; Praefcke and McMahon, 2004). GTP-γ-S is a non-hydrolyzable GTP analog that locks up dynamin and will prolong the response by impeding endocytosis (Takei et al., 1995; Yamashita et al., 2005). We tested the role of this pathway in endocytosis following the capacitance increase brought about by either voltage-gated Ca^{2+} influx or mitochondrial Ca^{2+}. Cultured bag cell neuron capacitance was tracked under voltage-clamp at −80 mV and dialysis with intracellular salines (Cs^{+}-based for voltage-gated Ca^{2+} influx, K^{+}-based for mitochondrial Ca^{2+}) supplemented with 0.1 mM GTP or 1 mM GTP-γ-S. Delivery of the 5-Hz, 1-min train elicited essentially the same capacitance change in control (n = 6) vs GTP-γ-S (n = 6) dialyzed neurons (Fig. 8A), with no statistical difference in magnitude or rate of recovery (Fig. 8B). On the contrary, the increase in capacitance induced by 20 μM FCCP was altered in neurons dialyzed with GTP-γ-S (n = 8) compared to GTP (n = 14) (Fig. 8C). This manifested as a near doubling of the response itself (Fig. 8D, left), as well as more gradual membrane retrieval, with approximately 25% less recovery at 5 min with GTP-γ-S (Fig. 8D, right).

Neurons from animal cohorts engaged in egg-laying behavior display a larger change in capacitance

The role of bag cell neuron secretion is to bring about ovulation (Conn and Kaczmarek, 1989). To acquire a better understanding of how the capacitance increase of single neurons relates to behavior, we compared the magnitude of the train-induced response in neurons from a cohort of animals that showed evidence of egg-laying vs a cohort that was not reproductively active. *Aplysia* are seasonal breeders and most often found to be mating and/or laying eggs from late-June through September (Audesirk, 1979). The egg-laying cohort was supplied to our laboratory in late-July, the peak of the *Aplysia* breeding season (Kupfermann, 1970; Audesirk, 1979), and daily observations routinely found egg masses in their tank, whereas the non-egg-laying cohort was harvested in early-June and presented no evidence of eggs. Bag cell neurons were regularly cultured from both cohorts and the capacitance tracked in randomly selected neurons throughout the time the animals were housed in our facility. Under voltage-clamp in Ca^{2+}-Cs^{+}-TEA ASW with Cs^{+}-based intracellular saline, a 5-Hz, 1-min train caused a larger capacitance change in egg-laying cohort neurons (n = 10) as opposed to non-egg-laying cohort neurons (n = 9) (Fig. 9A). Specifically, the average response was 5-fold greater and significantly different (Fig. 9B). Note, the majority of neurons considered in Figs. 1–8 were cultured from animals harvested during the breeding season, i.e., late-June through to September (Audesirk, 1979). Thus, egg-laying was anecdotally evident in these other animals, although the presence of egg masses was not tracked daily.

DISCUSSION

Bag cell neurons undergo an afterdischarge characterized by intracellular Ca^{2+} elevation and the secretion of neuropeptides to induce reproduction (Stuart et al., 1980; Kaczmarek et al., 1982; Woolum and Strumwasser, 1988; Fisher et al., 1994). Arch (1972) employed ^{3}H protein-labeling to show that an afterdischarge or high-K^{+} releases peptide, but only in the presence of extracellular Ca^{2+}. Similarly, Loechner et al. (1990) used high-pressure liquid chromatography to demonstrate that blocking voltage-gated Ca^{2+} channels during an afterdischarge suppresses peptide secretion. Finally, Hatcher et al. (2005) and Jo et al. (2007) detected the release of ELH and other peptides by mass spectrometry after driving action potentials in cultured bag cell neurons with either intracellular stimulation or high-K^{+}. In the present study, we monitored peptide secretion from individual bag cell neurons by tracking electrical capacitance – a well-established method to quantify vesicle fusion as a

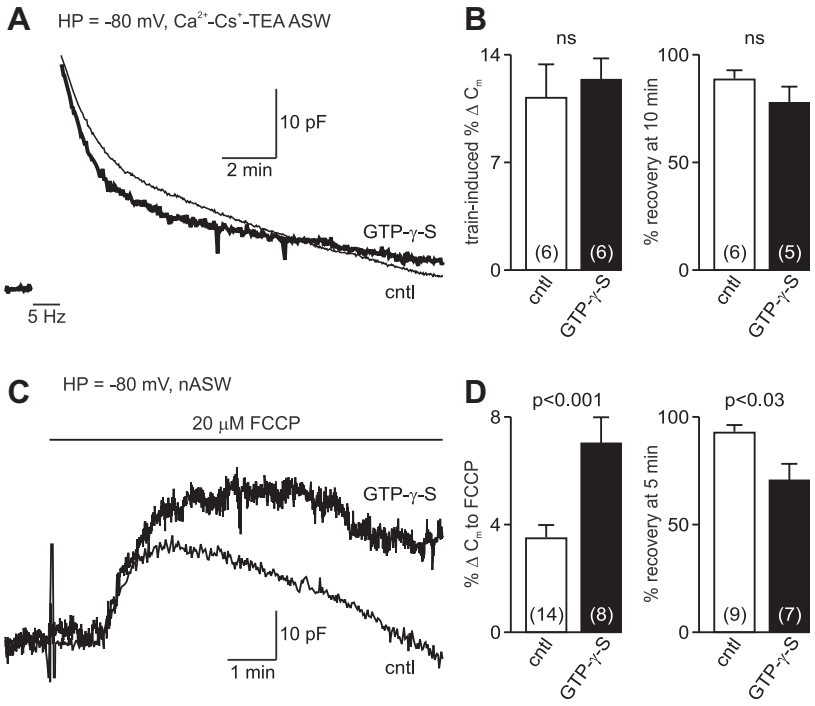

Fig. 8. GTP-γ-S alters the change in capacitance brought about by mitochondrial Ca^{2+} but not voltage-gated Ca^{2+}. (A) Tracking capacitance of two different neurons under whole-cell voltage-clamp at −80 mV in Ca^{2+}-Cs^{+}-TEA ASW with Cs^{+}-based intracellular saline. There is little difference in the magnitude or time course of the 5-Hz, 1-min train-evoked capacitance change following a 15-min dialysis with regular Cs^{+}-based intracellular saline containing 0.1 mM GTP (lighter trace, cntl) or when 1 mM GTP-γ-S is added to the intracellular saline (darker trace, GTP-γ-S). Scale bars apply to both traces. (B) Left panel, summary data show no significant difference between control and GTP-γ-S dialyzed neurons in the mean percent change of membrane capacitance due to Ca^{2+} influx from the train (two-tailed unpaired *t*-test). Right panel, the average percent recovery by 10 min of the capacitance change following the train is also not different between control and GTP-γ-S intracellular conditions (two-tailed unpaired *t*-test). (C) The capacitance traces of two separate neurons under whole-cell voltage-clamp at −80 mV in nASW with K^{+}-based intracellular saline are overlaid. The extent and duration of the change in membrane capacitance initiated by 20 μM FCCP are greater when the neuron is dialyzed with 1 mM GTP-γ-S (darker trace, GTP-γ-S) vs 0.1 mM GTP (lighter trace, cntl). Scale bars apply to both traces. (D) Left panel, summary data of the mean percent change in membrane capacitance to mitochondrial Ca^{2+} liberated with FCCP reveal a significant increase in response amplitude following GTP-γ-S dialysis compared to control (two-tailed unpaired *t*-test, Welch corrected). Right panel, the average percent recovery by 5 min of the FCCP-induced capacitance change shows a significantly slower reaction when GTP-γ-S is introduced into the neurons (two-tailed unpaired *t*-test, Welch corrected). The differences in *n*-values between the change in capacitance groups and the recovery-time groups reflect that some cells were lost before they recovered the full 5 min after FCCP application, and thus were not included in the recovery-time analysis.

change in plasma membrane area (Neher and Marty, 1982; Lim et al., 1990; Klyachko and Jackson, 2002; Yamashita et al., 2005).

Consistent with voltage-gated Ca^{2+} entry being the primary trigger for exocytosis (Katz and Miledi, 1967; Llinás et al., 1981), substituting Ba^{2+} for external Ca^{2+} or adding Ni^{2+} abolishes the train-induced capacitance increase in bag cell neurons. Ca^{2+} removal or Ca^{2+} channel block also eliminates peptide release from AtT20 and B-cells, as well as pituitary and hypothalamic neuroendocrine cells (Hsu and Jackson, 1996; Branchaw et al., 1998; Whim and Moss, 2001; Sedej et al., 2004; Soldo et al., 2004). That Ba^{2+} is ineffective at initiating bag cell neuron exocytosis concurs with Ba^{2+} substituting poorly for Ca^{2+} in transmitter release (Miledi, 1966; Nowycky et al., 1998; Shin et al., 2003). Yet, in the intact bag cell neuron cluster, Ba^{2+} can evoke ELH secretion, although this is likely due to Ba^{2+}-induced Ca^{2+}-release from intracellular stores, particularly in the processes (Fisher et al., 1994; Wayne et al., 1998). This discrepancy may be explained by our use of EGTA in the recording pipette, which would have prevented somatic Ca^{2+}- or Ba^{2+}-induced Ca^{2+}-release (Groten et al., 2013). Finally, we find that dsRNA knock-down of ELH expression diminishes the capacitance response. To the best of our knowledge, there are no examples of reduced peptide expression impacting neuronal secretion; however, dsRNA-inhibition of endothelin, *Drosophila* insulin-like peptide, or tumor necrosis factor alpha, decreases constitutive or inflammation-evoked secretion from non-neuronal cells (Rayhman et al., 2008; Colombani et al., 2012; Pichu et al., 2012). Attenuation of the capacitance change by reduced ELH expression may result from fewer vesicles being available for release by Ca^{2+} influx.

Although most of the neurons used throughout the present study had neurites, sprouting was not absolutely necessary for the train-induced capacitance increase. *In vivo*, bag cell neuron somata contain both large and small ELH-positive dense core vesicles, whereas the processes house only small peptidergic vesicles (Kreiner et al., 1986); in addition, α- and γ-bag cell peptide-containing vesicles are more prevalent in the soma (Fisher et al., 1988). Because our recordings are solely from the soma, the capacitance measurements are likely dominated by the fusion of soma-specific

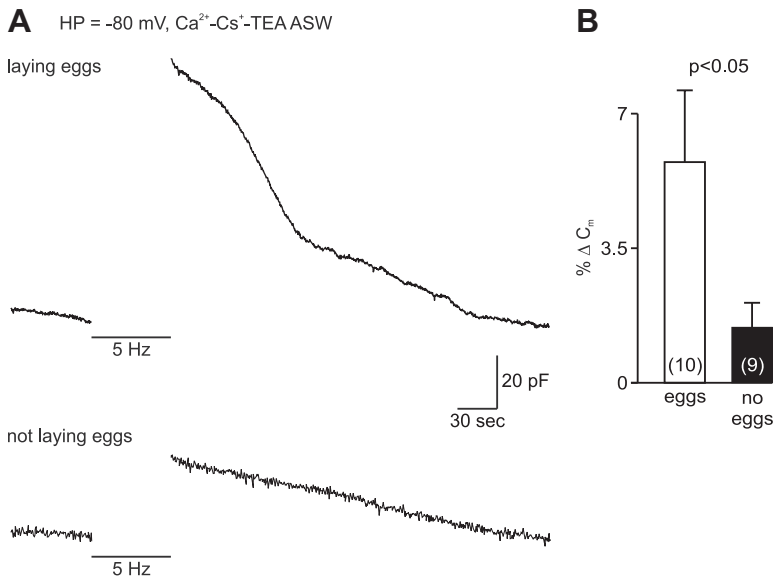

Fig. 9. Egg-laying animals yield neurons which show a greater increase in membrane capacitance. (A) Capacitance tracking from two different neurons whole-cell voltage-clamped to −80 mV in Ca^{2+}-Cs^{+}-TEA ASW and dialyzed with Cs^{+}-based intracellular saline. Upper trace, Stimulation with a 5-Hz, 1-min train of a neuron cultured from an animal in a cohort observed to be laying eggs results in a clear elevation of membrane capacitance. Lower trace, the same stimulus given to a neuron cultured from an animal whose cohort was not laying eggs presents a much smaller change in capacitance. Scale bars apply to both traces.(B) Summary data show a significantly greater average percent increase in capacitance evoked by the 5-Hz, 1-min train in neurons from egg-laying animals as compared to those from non-egg-laying animals (two-tailed Mann–Whitney test).

vesicles. Thus, our secretory responses may differ from the intact cluster, which clearly involves release from processes (Lee and Wayne, 2004). Nevertheless, secretion of bona fide ELH has been found using mass spectrometry of beads placed either directly on cultured bag cell neuron neurites or somata as well as directly on the intact cluster (Hatcher et al., 2005; Hatcher and Sweedler, 2008). Also, peptide release from sites other than the terminal is not unusual for neuroendocrine cells; for example, Pow and Morris (1989) first demonstrated that hypothalamic neurons release oxytocin and vasopressin from both the soma and dendrites.

Following vesicle fusion, the SNARE (soluble N-ethylmaleimide-sensitive factor (NSF) attachment protein receptor) complex is unravelled by the ATPase function of NSF (May et al., 2001; Rettig and Neher, 2002; Smith et al., 2008). NEM alkylates NSF and hinders peptide secretion from B-, AtT20, Chinese hamster ovary, and PC12 cells (Block et al., 1988; Chavez et al., 1996; Eliasson et al., 1997; Han et al., 1999). Exposure of bag cell neurons to NEM reduces the capacitance increase evoked by the train. This could be attributed to NSF alkylation, although NEM is also capable of alkylating Ca^{2+} channels (Fryer, 1992). However, we do not observe a significant effect of NEM on either the bag cell neuron Ca^{2+} current (this study) or a Ca^{2+}-influx-gated cation current (Hickey et al., 2010).

Classical neurotransmitter release occurs in a few hundred microseconds and requires considerable Ca^{2+} near the vesicle (Llinás et al., 1981; Adler et al., 1991). Generally, peptide release takes several milliseconds to seconds, necessitates sustained Ca^{2+}, and is reduced by the slow Ca^{2+} buffer, EGTA (Smith et al., 1984; Neher, 1998). This is observed for the secretion of atrial natriuretic factor, growth hormone, insulin, oxytocin/vasopressin, and proopiomelanocortin (Lim et al., 1990; Thomas et al., 1993; Burke et al., 1997; Branchaw et al., 1998; Kilic et al., 2001; Barg et al., 2002; Sedej et al., 2004). Bag cell neuron exocytosis is reduced by EGTA and is steeply dependent on the pulse duration of the train. The capacitance change is first observed at a 37-ms pulse duration and plateaus by 50 ms. This despite Ca^{2+} current recordings showing trains with 10- or 25-ms pulse durations still produce Ca^{2+} influx. Furthermore, the duration for half-maximal Ca^{2+} influx is essentially 37 ms with a plateau at 75 ms. Thus, a Ca^{2+} threshold must be reached to engage a releasable pool of vesicles, suggesting low-affinity binding of Ca^{2+} to several targets, multiple Ca^{2+}-dependent reactions, and/or a lack of molecular coupling between Ca^{2+} channels and vesicles – the latter being supported by EGTA sensitivity (Thomas et al., 1993; Neher, 1998). Both oxytocin/vasopressin and proopiomelanocortin secretion share a similarly abrupt dependence on stimulus duration, with proopiomelanocortin release also presenting a high Ca^{2+} threshold which subsequently plateaus (Thomas et al., 1993; Soldo et al., 2004). The plateauing of bag cell neuron secretion may represent both a levelling off of Ca^{2+} influx with increasing pulse duration as well as competition between exocytosis and endocytosis.

Peptide secretion typically depresses to repeated stimulation (Thomas et al., 1993; Hsu and Jackson, 1996; Whim et al., 1997; Kilic et al., 2001; Soldo et al., 2004). Bag cell neuron exocytosis fatigues markedly, with the capacitance increase dropping by half following a second stimulus. This is likely not due to whole-cell

run-down (Ammälä et al., 1993), given that we observed robust responses to a single train following dialysis for a similar time period as the double train experiments. Interestingly, Arch (1972) reported that following high-K^+-induced peptide release from intact bag cell neurons, delivering high-K^+ again elicited only one-fifth the amount of secretion, and a third stimulus produced no effect. Burke et al. (1997) suggest that repletion of atrial natriuretic factor-containing vesicles is restricted to a small proportion of slow-moving granules. ELH-containing vesicles are approximately 150 nm in diameter (Fisher et al., 1988), and depression could reflect the limited mobility of large vesicles in the reserve pool to replenish the releasable pool.

Bag cell neurons appear unique, in that liberating mitochondrial Ca^{2+} with FCCP directly provokes peptide exocytosis. The only exception we have found is FCCP-induced catecholamine secretion from chromaffin cells (Miranda-Ferreira et al., 2009). In hippocampal, superior olivary complex, and crayfish neurons, liberating mitochondrial Ca^{2+} or preventing uptake does not cause transmitter release, but can disrupt short-term plasticity (Tang and Zucker, 1997; Billups and Forsythe, 2002; Lee et al., 2007). In part, the pool of bag cell neuron releasable vesicles appears to be shared among voltage-gated Ca^{2+} and mitochondrial Ca^{2+}. Perhaps, in the absence of molecular coupling between Ca^{2+} channels and vesicles, any large Ca^{2+} elevation is sufficient to bring about exocytosis. Bag cell neuron Ca^{2+}-induced Ca^{2+}-release requires uptake and subsequent release of Ca^{2+} from the mitochondria (Geiger and Magoski, 2008; Groten et al., 2013); moreover, activity- or Ca^{2+}-induced Ca^{2+}-release following an afterdischarge prolongs secretion from the intact cluster (Wayne et al., 1998). The latter may involve Ca^{2+} from intracellular stores in the processes (Michel and Wayne, 2002), a region known to contain abundant mitochondria (White and Kaczmarek, 1997). Thus, the physiological liberation of mitochondrial Ca^{2+} could promote ELH secretion *in vivo*.

Endoplasmic reticulum Ca^{2+} does not trigger bag cell neuron secretion, since CPA has no effect on capacitance. This is in-keeping with Jonas et al. (1997), who did not observe release from intact bag cell neurons following exposure to thapsigargin, a CPA analog (Thastrup et al., 1990). Likewise, Gilbert et al. (2008) reported that insulin secretion is not evoked by endoplasmic reticulum Ca^{2+}; however, other work shows Ca^{2+} from this store potentiates or causes the secretion of atrial natriuretic factor, luteinizing hormone, and oxytocin (Tse et al., 1997; Ludwig et al., 2002; Shakiryanova et al., 2007). In the bag cell neurons, the secretory capacity of the endoplasmic reticulum may be influenced by the fact that these organelles appear to have less stored Ca^{2+} than the mitochondria (Hickey et al., 2010). Furthermore, we recently demonstrated that mitochondria, but not the endoplasmic reticulum, sequester voltage-gated Ca^{2+} influx, which may indicate the former are closer to the membrane and the readily releasable pool (Groten et al., 2013).

Endocytotic retrieval following exocytosis is reflected by a decrease in capacitance (Neher and Marty, 1982). GTP-γ-S disrupts endocytosis by locking up the GTPase, dynamin (Takei et al., 1995; Praefcke and McMahon, 2004; Yamashita et al., 2005). However, GTP-γ-S fails to alter bag cell neuron exocytosis or subsequent endocytosis when stimulated by Ca^{2+} entry. Intense Ca^{2+} influx at peptidergic and classical transmitter release sites can lead to GTP-γ-S-insensitive endocytosis (Engisch and Nowycky, 1998; Zhang et al., 2004; Clayton et al., 2008; Xu et al., 2008). Conversely, the FCCP-induced secretion is both enhanced, and the recovery slowed, by GTP-γ-S. While this may suggest differences in membrane retrieval following rapid vs slow exocytosis, additional mechanisms may be at work, given that GTP-γ-S can turn on Ras-like GTPases and alter the localization of mitochondria or directly influence exocytosis (Reis et al., 2009; Ory and Gasman, 2011).

The capacitance changes in cultured bag cell neurons are consistent with exocytosis produced by Ca^{2+} entry or Ca^{2+} liberated from mitochondria. The secretory response has a high Ca^{2+} threshold, which could reflect a Ca^{2+}-dependent preparatory step prior to exocytosis (Nowycky et al., 1998). Such an arrangement is not unexpected for the secretion of a hormone that controls an energetically expensive and vulnerable activity like egg-laying. This is reinforced by our finding that egg-laying animals yield neurons which secrete substantially more to the train. The breeding season is associated with both greater ELH synthesis in the bag cell neurons and a more reliable induction of egg-laying following ELH injection (Kupfermann, 1970; Berry, 1982). Thus, neurons from non-breeding animals could have fewer peptidergic vesicles available for release. Alternatively, the extent of Ca^{2+} influx could differ between the two neuronal groups. In a subset of cells from Fig. 9, preliminary intracellular Ca^{2+} measurements using whole-cell fura PE3 imaging (see Groten et al., 2013 for methods), revealed that the train-elicited change in the fura ratio of neurons cultured from non-egg-laying animals (0.28 ± 0.08; $n = 9$) was significantly smaller compared to those from egg-laying animals (0.71 ± 0.06; $n = 8$) ($p < 0.001$, two-tailed unpaired *t*-test). This has parallels to Nick et al. (1996), who showed juvenile *Aplysia*, which typically do not lay eggs, also have small Ca^{2+} currents. Still, we cannot rule out the possibility that the time of year or exact location of animal collection could influence secretion. In general, the neuroendocrine control of fundamental behaviors, like egg-laying, may require multiple Ca^{2+} sources and a high threshold to ensure appropriate execution.

Acknowledgements—The authors thank S.L. Smith and H.M. Fuller-Hodgson for technical assistance, N.L. Wayne for the generous gift of ELH antibody, N.M. Magoski for the evaluation of previous drafts of the manuscript, and the anonymous Reviewers for providing constructive comments to improve the manuscript. C.M.H. and C.J.G. held Ontario Graduate Scholarships. C.J.G. holds a Natural Sciences and Engineering Research Council Post-graduate Scholarship. N.S.M. holds a Canadian Institutes

of Health Research New Investigator Award. Supported by a CIHR operating grant to NSM.

REFERENCES

Adler EM, Augustine GJ, Duffy SN, Charlton MP (1991) Alien intracellular calcium chelators attenuate neurotransmitter release at the squid giant synapse. J Neurosci 11:1496–1507.

Ammälä C, Eliasson L, Bokvist K, Larsson O, Ashcroft FM, Rorsman P (1993) Exocytosis elicited by action potentials and voltage-clamp calcium currents in individual mouse pancreatic B-cells. J Physiol 472:665–688.

Arch S (1972) Polypeptide secretion from the isolated parietovisceral ganglion of *Aplysia californica*. J Gen Physiol 59:47–59.

Audesirk TE (1979) A field study of growth and reproduction in *Aplysia californica*. Biol Bull 157:407–421.

Babcock DF, Herrington J, Goodwin PC, Park TB, Hille B (1997) Mitochondrial participation in the intracellular Ca^{2+} network. J Cell Biol 136:833–844.

Barg S, Olofsson CS, Schriever-Abelin J, Wendt A, Gebre-Medhin S, Renstrom E, Rorsman P (2002) Delay between fusion pore opening and peptide release from large dense-core vesicles in neuroendocrine cells. Neuron 33:287–299.

Berry RW (1982) Seasonal modulation of synthesis of the neurosecretory egg-laying hormone of *Aplysia*. J Neurobiol 13:327–335.

Bhargava A, Dallman MF, Pearce D, Choi S (2004) Long double-stranded RNA-mediated RNA interference as a tool to achieve site-specific silencing of hypothalamic neuropeptides. Brain Res Protoc 13:115–125.

Bicknell RJ, Leng G (1981) Relative efficiency of neural firing patterns for vasopressin release *in vitro*. Neuroendocrinol 33:295–299.

Billups B, Forsythe ID (2002) Presynaptic mitochondrial calcium sequestration influences transmission at mammalian central synapses. J Neurosci 22:5840–5847.

Block MR, Glick BS, Wilcox CA, Wieland FT, Rothman JE (1988) Purification of an N-ethylmaleimide-sensitive protein catalyzing vesicular transport. Proc Natl Acad Sci U S A 85:7852–7856.

Bowman EJ, Siebers A, Altendorf K (1988) Bafilomycins: a class of inhibitors of membrane atpases from microorganisms, animal cells, and plant cells. Proc Natl Acad Sci U S A 85:7972–7976.

Branchaw JL, Hsu S-F, Jackson MB (1998) Membrane excitability and secretion from peptidergic nerve terminals. Cell Mol Neurobiol 18:45–63.

Brown RO, Pulst SM, Mayeri E (1989) Neuroendocrine bag cells of *Aplysia* are activated by bag cell peptide-containing neurons in the pleural ganglion. J Neurophysiol 61:1142–1152.

Burke NV, Han W, Li D, Takimoto K, Watkins SC, Levitan ES (1997) Neuronal peptide release is limited by secretory granule mobility. Neuron 19:1095–1102.

Byerly L, Chase BP, Stimers JR (1985) Permeation and interaction of divalent cations in calcium channels of snail neurons. J Gen Physiol 85:491–518.

Chavez RA, Miller SG, Moore HP (1996) A biosynthetic regulated secretory pathway in constitutive secretory cells. J Cell Biol 133:1177–1191.

Chiu AY, Stumwasser F (1981) An immunohistochemical study of the neuropeptidergic bag cells of *Aplysia*. J Neurosci 8:812–826.

Chiu AY, Hunkapiller MW, Heller E, Stuart DK, Hood LE, Strumwasser F (1979) Purification and primary structure of the neuropeptide egg-laying hormone of *Aplysia californica*. Proc Natl Acad Sci U S A 76:6656–6660.

Christensen KA, Myers JT, Swanson JA (2002) PH-dependent regulation of lysosomal calcium in macrophages. J Cell Sci 115:599–607.

Clayton EL, Evans GJO, Cousin MA (2008) Bulk synaptic vesicle endocytosis is rapidly triggered during strong stimulation. J Neurosci 28:6627–6632.

Colombani J, Andersen DS, Léopold P (2012) Secreted peptide Dilp8 coordinates *Drosophila* tissue growth with developmental timing. Science 336:582–585.

Conn PJ, Kaczmarek LK (1989) The bag cell neurons of *Aplysia*. Mol Neurobiol 3:237–273.

Dreifuss JJ, Kalnins I, Kelly JS, Ruf KB (1971) Action potentials and release of neurohypophysial hormones *in vitro*. J Physiol 215:805–817.

Dudek FE, Tobe SS (1978) Bag cell peptide acts directly on ovotestis of *Aplysia californica*: basis for an *in vitro* bioassay. Gen Comp Endocrinol 36:618–627.

Dudek FE, Cobbs JS, Pinsker HM (1979) Bag cell electrical activity underlying spontaneous egg laying in freely behaving *Aplysia brasiliana*. J Neurophysiol 42:804–817.

Eliasson L, Renström E, Ding WG, Proks P, Rorsman P (1997) Rapid ATP-dependent priming of secretory granules precedes Ca^{2+}-induced exocytosis in mouse pancreatic B-cells. J Physiol 503:399–412.

Engisch KL, Nowycky MC (1998) Compensatory and excess retrieval: two types of endocytosis following single step depolarizations in bovine adrenal chromaffin cells. J Physiol 506:591–608.

Ferguson GP, Ter Maat A, Parsons DW, Pinsker HM (1989) Egg laying in *Aplysia*. I. Behavioral patterns and muscle activity of freely behaving animals after selectively elicited bag cell discharges. J Comp Physiol A 164:8358.

Fieber LA (1995) Characterization and modulation of Na^+ and Ca^{2+} currents underlying the action potential in bag cells of two species of *Aplysia*. J Exp Biol 198:2337–2347.

Fire A, Xu SQ, Montgomery MK, Kostas SA, Driver SE, Mello CC (1998) Potent and specific genetic interference by double-stranded RNA in *Caenorhabditis elegans*. Nature 391:806–811.

Fisher JM, Sossin W, Newcomb R, Scheller RH (1988) Multiple neuropeptides derived from a common precursor are differentially packaged and transported. Cell 54:813–822.

Fisher TE, Levy S, Kaczmarek LK (1994) Transient changes in intracellular calcium associated with a prolonged increase in excitability in neurons of *Aplysia californica*. J Neurophysiol 71:1254–1257.

Fryer MW (1992) An N-ethylmaleimide-sensitive G-protein modulates *Aplysia* Ca^{2+} channels. Neurosci Lett 146:84–86.

Gainer H, Wolfe SA, Obaid AL, Salzberg BM (1986) Action potentials and frequency-dependent secretion in the mouse neurohypophysis. Neuroendocrinology 43:557–563.

Gardam KE, Geiger JE, Hickey CM, Hung AY, Magoski NS (2008) Flufenamic acid affects multiple currents and causes intracellular Ca^{2+} release in *Aplysia* bag cell neurons. J Neurophysiol 100:38–49.

Geiger JE, Magoski NS (2008) Ca^{2+}-induced Ca^{2+}-release in *Aplysia* bag cell neurons requires interaction between mitochondrial and endoplasmic reticulum stores. J Neurophysiol 100:24–37.

Geiger JE, Hickey CM, Magoski NS (2009) Ca^{2+} entry through a non-selective cation channel in *Aplysia* bag cell neurons. Neuroscience 162:1023–1038.

Gilbert M, Seung-Ryoung Jung S-R, Reed BJ, Sweet IR (2008) Islet oxygen consumption and insulin secretion tightly coupled to calcium derived from l-type calcium channels but not from the endoplasmic reticulum. J Biol Chem 283:24334–24342.

Gillis KD (1995) Techniques for membrane capacitance measurements. In: Single channel recording, 2nd edn. Sakmann B, Neher E eds, pp 155–197, Plenum Press.

Goncalves PP, Meireles SM, Neves P, Vale MG (1999) Synaptic vesicle Ca^{2+}/H^+ antiport: dependence on the proton electrochemical gradient. Mol Brain Res 71:178–184.

Groten CJ, Rebane JT, Blohm G, Magoski NS (2013) Separate Ca^{2+} sources are buffered by distinct Ca^{2+} handling systems in *Aplysia* neuroendocrine cells. J Neurosci 33:6476–6491.

Hagiwara S, Fukuda J, Eaton DC (1974) Membrane currents carried by Ca, Sr, and Ba in barnacle muscle fiber during voltage clamp. J Gen Physiol 63:564–578.

Han W, Li D, Stout AK, Takimoto H, Levitan ES (1999) Ca^{2+}-induced deprotonation of peptide hormones inside secretory vesicles in preparation for release. J Neurosci 19:900–905.

Hartzell HC (1981) Mechanisms of slow postsynaptic potentials. Nature 291:539–544.

Hatcher NG, Sweedler JV (2008) *Aplysia* bag cells function as a distributed neurosecretory network. J Neurophysiol 99: 333–343.

Hatcher NG, Richmond TA, Rubakhin SS, Sweedler JV (2005) Monitoring activity-dependent peptide release from the CNS using single-bead solid-phase extraction and MALDI TOF MS detection. Anal Chem 77:1580–1587.

Heytler PG, Prichard WW (1962) A new class of uncoupling agents – carbonyl cyanide phenylrydrazones. Biochem Biophys Res Commun 7:272–275.

Hickey CM, Geiger KE, Groten CJ, Magoski NS (2010) Mitochondrial Ca^{2+} activates a cation current in *Aplysia* bag cell neurons. J Neurophysiol 103:1543–1556.

Hille B (2001) Ionic channels of excitable membranes. Sinauer Associates.

Hsu S-F, Jackson MB (1996) Rapid exocytosis in the nerve terminals of the rat posterior pituitary. J Physiol 494:539–553.

Hung AY, Magoski NS (2007) Activity-dependent initiation of a prolonged depolarization in *Aplysia* bag cell neurons: role for a cation channel. J Neurophysiol 97:2465–2479.

Jo K, Heien ML, Thompson LB, Zhong M, Nuzzo RG, Sweedler JV (2007) Mass spectrometric imaging of peptide release from neuronal cells within microfluidic devices. Lab Chip 7:1454–1460.

Jonas EA, Knox RJ, Smith TCM, Wayne NL, Connor JA, Kaczmarek LK (1997) Regulation by insulin of a unique neuronal Ca^{2+} pool and neuropeptide secretion. Nature 385:343–346.

Kachoei BA, Knox RJ, Uthuza D, Levy S, Kaczmarek LK, Magoski NS (2006) A store-operated Ca^{2+} influx pathway in the bag cell neurons of *Aplysia*. J Neurophysiol 96:2688–2698.

Kaczmarek LK, Jennings K, Strumwasser F (1982) An early sodium and a late calcium phase in the afterdischarge of peptide-secreting neurons of *Aplysia*. Brain Res 238:105–115.

Katz B, Miledi R (1967) The timing of calcium action during neuromuscular transmission. J Physiol 189:535–544.

Kilic G, Angleson JK, Cochilla AJ, Nussinovitch I, Betz WJ (2001) Sustained stimulation of exocytosis triggers continuous membrane retrieval in rat pituitary somatotrophs. J Physiol 532:771–783.

Klyachko VA, Jackson MB (2002) Capacitance steps and fusion pores of small and large-dense-core vesicles in nerve terminals. Nature 418:89–92.

Knox RJ, Jonas EA, Kao L-S, Smith PJS, Connor JA, Kaczmarek LK (1996) Ca^{2+} influx and activation of a cation current are coupled to intracellular Ca^{2+} release in peptidergic neurons of *Aplysia californica*. J Physiol 494:627–693.

Kreiner T, Sossin W, Scheller RH (1986) Localization of *Aplysia* neurosecretory peptides to multiple populations of dense core vesicles. J Cell Biol 102:769–782.

Kupfermann I, Weiss KR (1978) The command neuron concept. Behav Brain Sci 1:3–39.

Kupfermann I (1967) Stimulation of egg laying: possible neuroendocrine function of bag cells of abdominal ganglion of *Aplysia californica*. Nature 216:814–815.

Kupfermann I (1970) Stimulation of egg laying by extracts of neuroendocrine cells (bag cells) of abdominal ganglion of *Aplysia*. J Neurophysiol 33:877–881.

Lee W, Wayne NL (2004) Secretion of locally synthesized neurohormone from neurites of peptidergic neurons. J Neurochem 88:532–537.

Lee D, Lee K-H, Ho W-K, Lee S-H (2007) Target cell-specific involvement of presynaptic mitochondria in post-tetanic potentiation at hippocampal mossy fiber synapses. J Neurosci 27:13603–13613.

Lee Y-S, Choia S-L, Lee S-H, Kim H, Park H, Lee N, Lee S-H, Chae Y-S, Jang D-J, Kandel ER, Kaang BK (2009) Identification of a serotonin receptor coupled to adenylyl cyclase involved in learning-related heterosynaptic facilitation in *Aplysia*. Proc Natl Acad Sci U S A 106:14634–14639.

Lim NF, Nowycky MC, Bookman RJ (1990) Direct measurement of exocytosis and calcium currents in single vertebrate nerve terminals. Nature 344:449–451.

Llinás R, Steinberg IZ, Walton K (1981) Relationship between presynaptic calcium current and postsynaptic potential in squid giant synapse. Biophys J 33:323–351.

Loechner KJ, Azhderian EM, Dreyer R, Kaczmarek LK (1990) Progressive potentiation of peptide release during a neuronal discharge. J Neurophysiol 63:738–744.

Loechner KJ, Knox RJ, Connor JA, Kaczmarek LK (1992) Hyperosmotic media inhibit voltage-dependent calcium influx and peptide release in *Aplysia* neurons. J Membr Biol 128:41–52.

Ludwig M, Sabatier N, Bull PM, Landgraf R, Dayanithi G, Leng G (2002) Intracellular calcium stores regulate activity-dependent neuropeptide release from dendrites. Nature 418:85–89.

Lupinsky DA, Magoski NS (2006) Ca^{2+}-dependent regulation of a non-selective cation channel from *Aplysia* bag cell neurones. J Physiol 575:491–506.

Magoski NS, Knox RJ, Kaczmarek LK (2000) Activation of a Ca^{2+}-permeable cation channel produces a prolonged attenuation of intracellular Ca^{2+} release in *Aplysia* bag cell neurones. J Physiol 522:271–283.

May AP, Whiteheart SW, Weis WI (2001) Unraveling the mechanism of the vesicle transport ATPase NSF, the N-ethylmaleimide-sensitive factor. J Biol Chem 276:21991–21994.

McFarlane MB, Gilly WF (1998) State-dependent nickel block of a high-voltage-activated neuronal calcium channel. J Neurophysiol 80:1678–1685.

Michel S, Wayne NL (2002) Neurohormone secretion persists after post-afterdischarge membrane depolarization and cytosolic calcium elevation in peptidergic neurons in intact nervous tissue. J Neurosci 22:9063–9069.

Miledi R (1966) Strontium as a substitute for calcium in the process of transmitter release at the neuromuscular junction. Nature 212:1233–1234.

Miranda-Ferreira R, de Pascual R, Caricati-Neto A, Gandía A, Jurkiewicz A, García AG (2009) Role of the endoplasmic reticulum and mitochondria on quantal catecholamine release from chromaffin cells of control and hypertensive rats. J Pharmacol Exp Ther 329:231–240.

Naraghi M (1997) T-jump study of calcium binding kinetics of calcium chelators. Cell Calcium 22:255–268.

Neher E, Marty A (1982) Discrete changes of cell membrane capacitance observed under conditions of enhanced secretion in bovine adrenal chromaffin cells. Proc Natl Acad Sci U S A 79:6712–6716.

Neher E, Sakaba T (2008) Multiple roles of calcium ions in the regulation of neurotransmitter release. Neuron 59:861–872.

Neher E (1998) Vesicle pools and Ca^{2+} microdomains: new tools for understanding their roles in neurotransmitter release. Neuron 20:389–399.

Newcomb R, Fisher JM, Scheller RH (1988) Processing of the egg-laying hormone (ELH) precursor in the bag cell neurons of *Aplysia*. J Biol Chem 263:12514–12521.

Nick TA, Kaczmarek LK, Carew TJ (1996) Ionic currents underlying developmental regulation of repetitive firing in *Aplysia* bag cell neurons. J Neurosci 16:7583–7598.

Nowycky MC, Seward EP, Chernevskaya NI (1998) Excitation-secretion coupling in mammalian neurohypophysial nerve terminals. Cell Mol Neurobiol 18:65–80.

Ory S, Gasman S (2011) Rho GTPases and exocytosis: what are the molecular links? Semin Cell Dev Biol 22:27–32.

Pichu S, Krishnamoorthy S, Zhang B, Jing Y, Shishkov A, Ponnappa BC (2012) Dicer-substrate siRNA inhibits tumor necrosis factor alpha secretion in Kupffer cells *in vitro*: *in vivo* targeting of Kupffer cells by siRNA-liposomes. Pharmacol Res 65:48–55.

Pow DV, Morris JF (1989) Dendrites of hypothalamic magnocellular neurons release neurohypophysial peptides by exocytosis. Neuroscience 32:435–439.

Praefcke GJK, McMahon HT (2004) The dynamin superfamily: universal membrane tubulation and fission molecules? Nat Rev Mol Cell Biol 5:133–147.

Rayhman O, Klipper E, Muller L, Davidson B, Reich R, Meidan R (2008) Synthesis and the invasive phenotype of ovarian carcinoma endothelin-converting enzyme-1 inhibit endothelin-1. Cancer Res 68:9265–9273.

Reis K, Fransson A, Pontus Aspenström (2009) The Miro GTPases: at the heart of the mitochondrial transport machinery. FEBS Lett 583:1391–1398.

Rettig J, Neher E (2002) Emerging roles of presynaptic proteins in Ca^{2+}-triggered exocytosis. Science 298:781–785.

Scheller RH, Jackson JF, McAllister LB, Rothman BS, Mayeri E, Axel R (1983) A single gene encodes multiple neuropeptides mediating a stereotyped behavior. Cell 32:7–22.

Sedej S, Tsujimoto T, Zorec R, Rupnik M (2004) Voltage-activated Ca^{2+} channels and their role in the endocrine function of the pituitary gland in newborn and adult mice. J Physiol 555: 769–782.

Seidler NW, Jona I, Vegh M, Martonosi A (1989) Cyclopiazonic acid is a specific inhibitor of the Ca^{2+}-ATPase of sarcoplasmic reticulum. J Biol Chem 264:17816–17823.

Shakiryanova D, Klose MK, Zhou Y, Gu T, Deitcher DL, Atwood HL, Hewes RS, Levitan ES (2007) Presynaptic ryanodine receptor-activated calmodulin kinase ii increases vesicle mobility and potentiates neuropeptide release. J Neurosci 27:7799–7806.

Shapiro MS, Wollmuth LP, Hille B (1994) Modulation of Ca^{2+} channels by PTX-sensitive G-proteins is blocked by N-ethylmaleimide in rat sympathetic neurons. J Neurosci 14:7109–7116.

Shin O-H, Rhee J-S, Tang J, Sugita S, Rosenmund C, Sudhof TC (2003) Sr^{2+} binding to the Ca^{2+} binding site of the synaptotagmin 1 C2b domain triggers fast exocytosis without stimulating SNARE interactions. Neuron 37:99–108.

Simpson PB, Russell JT (1996) Mitochondria support inositol 1,4,5-trisphosphate-mediated Ca^{2+} waves in cultured oligodendrocytes. J Biol Chem 271:33493–33501.

Smith PD, Liesegang GW, Berger RL, Czerlinski G, Podolsky RJ (1984) A stopped-flow investigation of calcium ion binding by ethylene glycol bis(β-aminoethyl ether)-N,N′-tetraacetic acid. Anal Biochem 143:188–195.

Smith SM, Renden R, von Gersdorff H (2008) Synaptic vesicle endocytosis: fast and slow modes of membrane retrieval. Trends Neurosci 31:559–568.

Soldo BI, Giovannucci DR, Stuenkel EL, Moises HC (2004) Ca^{2+} and frequency dependence of exocytosis in isolated somata of magnocellular supraoptic neurones of the rat hypothalamus. J Physiol 555:699–711.

Sossin WS, Fisher JM, Scheller RH (1990) Sorting within the regulated secretory pathway occurs in the trans-golgi network. J Cell Biol 110:1–12.

Stuart DK, Chiu AY, Strumwasser F (1980) Neurosecretion of egg-laying hormone and other peptides from electrically active bag cell neurons of *Aplysia*. J Neurophysiol 43:488–498.

Takei K, McPherson PS, Schmid SL, De Camilli P (1995) Tubular membrane invaginations coated by dynamin rings are induced by GTP-γS in nerve terminals. Nature 374:186–190.

Tam AKT, Geiger JE, Hung AY, Groten CJ, Magoski NS (2009) Persistent Ca^{2+} current contributes to a prolonged depolarization in *Aplysia* bag cell neurons. J Neurophysiol 102:3753–3765.

Tang Y-G, Zucker RS (1997) Mitochondrial involvement in post-tetanic potentiation of synaptic transmission. Neuron 18:483–491.

Thastrup O, Cullen PJ, Drobak BK, Hanley MR, Dawson AP (1990) Thapsigargin, a tumor promoter, discharges intracellular Ca^{2+} stores by specific inhibition of the endoplasmic reticulum Ca^{2+}-ATPase. Proc Natl Acad Sci U S A 87:2466–2470.

Thomas P, Wong JG, Lee AK, Almers W (1993) A low affinity Ca^{2+} receptor controls the final steps in peptide secretion from pituitary melanotrophs. Neuron 11:93–104.

Tse FW, Tse A, Hille B, Horstmann H, Almers W (1997) Local Ca^{2+} release from internal stores controls exocytosis in pituitary gonadotrophs. Neuron 18:121–132.

Van Der Bliek AM, Meyerowitz EM (1991) Dynamin-like protein encoded by the *Drosophila* shibire gene associated with vesicular traffic. Nature 351:411–414.

Van Kesteren RE, Carter C, Dissel HMG, Van Minnen J, Gouwenberg Y, Syed NI, Spencer GE, Smit AB (2006) Local synthesis of actin-binding protein β-thymosin regulates neurite outgrowth. J Neurosci 26:152–157.

Wayne NL, Kim YJ, Lee W (1998) Prolonged hormone secretion from neuroendocrine cells of *Aplysia* is independent of extracellular calcium. J Neuroendocrinol 10:529–537.

Whim MD, Moss GWJ (2001) A novel technique that measures peptide secretion on a millisecond timescale reveals rapid changes in release. Neuron 30:37–50.

Whim MD, Niemann H, Kaczmarek LK (1997) The secretion of classical and peptide cotransmitters from a single presynaptic neuron involves a synaptobrevin-like molecule. J Neurosci 17:2338–2347.

White BH, Kaczmarek LK (1997) Identification of a vesicular pool of calcium channels in the bag cell neurons of *Aplysia californica*. J Neurosci 17:1582–1595.

White SH, Magoski NS (2012) Acetylcholine-evoked afterdischarge in *Aplysia* bag cell neurons. J Neurophysiol 107:2672–2685.

Wickner W, Schekman R (2008) Membrane fusion. Nat Struc Mol Biol 15:658–664.

Woolum JC, Strumwasser F (1988) Calcium changes in isolated peptidergic neurons during activation by a cAMP analog. Brain Res 444:1–9.

Xu J, McNeil B, Wu W, Nees D, Bai L, Wu L-G (2008) GTP-independent rapid and slow endocytosis at a central synapse. Nat Neurosci 11:45–53.

Yamashita T, Hige T, Takahashi T (2005) Vesicle endocytosis requires dynamin-dependent GTP hydrolysis at a fast CNS synapse. Science 307:124–127.

Zhang C, Xiong W, Zheng H, Wang L, Lu B, Zhou Z (2004) Calcium- and dynamin-independent endocytosis in dorsal root ganglion neurons. Neuron 42:225–236.

(Accepted 11 July 2013)
(Available online 19 July 2013)